

# Decision support for the selection of optimal tower site locations for early-warning wildfire detection systems in South Africa

Andries Heyns<sup>a,b,\*</sup>, Warren du Plessis<sup>c</sup>, Kevin M. Curtin<sup>b</sup>, Michael Kosch<sup>d,e,f,g</sup>, Gavin Hough<sup>g</sup>

<sup>a</sup>Humanitarian Logistics and Supply Chain Research Institute, Hanken School of Economics, Helsinki, Finland

<sup>b</sup>Laboratory for Location Science, Department of Geography, University of Alabama, USA

<sup>c</sup>University of Pretoria, Pretoria, South Africa

<sup>d</sup>South African National Space Agency, Hermanus, South Africa

<sup>e</sup>Department of Physics, Lancaster University, Lancaster, UK

<sup>f</sup>University of Western Cape, Bellville, South Africa

<sup>g</sup>EnviroVision Solutions, Durban, South Africa

\* Corresponding author, contactable at andries.heyns@hanken.fi

## Abstract

Effective early detection of forest fires can be achieved by specialised systems of tower-mounted cameras. Foresters and locals with intimate knowledge of the terrain traditionally plan the tower site locations – without the aid of computational optimisation tools. However, such knowledge and expertise may not be available to system planners when entering vast new territories. The process of selecting multiple tower sites from a large number of potential site locations with the aim of maximising system visibility of smoke above a prescribed region is a complex combinatorial optimisation problem. We present two recent applications of novel site-selection frameworks for tower-mounted *camera-based wildfire detection systems* (CWDS), which have been under development with guidance from experts from the South African-developed *ForestWatch* wildfire detection system. A novel single-site search framework determined alternatives for thirteen proposed sites in South Africa's Mpumalanga province, of which 6 alternatives were chosen over the initially proposed sites. The system-site selection framework was showcased in determining a four-camera CWDS layout in South Africa's Southern Cape – drastically improving on the detection capability of the layout initially proposed by technical experts.

Keywords: facility location, maximal cover, optimisation, wildfire

## 1 Introduction

Unexpected and uncontrolled wildfires spread rapidly and often turn into devastating natural disasters that affect the environment, ecosystems, economies and societies the world over. South Africa is no exception and suffers significant wildfire damage every year (Strydom and Savage, 2016). Wildfires are not only a threat to homes, families, and infrastructure, but also to the forestry assets of the South African timber industry. The South African forest sector employs roughly 165 900 workers and provides livelihood support to 652 000 of the country's rural population, and the government-run *Forestry Livelihoods Programme* is contributing to eradicating poverty (South African Government, 2009). A large percentage of South Africa's population is located in rural areas in these fire-prone forested regions and are especially vulnerable. It follows that the earliest possible detection of a wildfire is of critical importance. The sooner it is detected, the sooner suppressing action can be taken and the more manageable the size of the fire may be (Rego and Catry, 2006) – potentially minimising the loss of life, the scale of destruction, and the overall damage to the timber industry and affected livelihoods.

Early wildfire detection can effectively be achieved by *camera-based wildfire detection systems* (CWDSs) which comprise a number of specialised cameras that monitor the surrounding environment for smoke (Heyns et al., 2019; Martell, 2015). The cameras are mounted on top of towers that provide an elevated viewpoint above the terrain surface, resulting in improved visibility of the surrounding environment. Figure 1(a) shows a typical camera, while in Figure 1(b) a 32-m tower with a camera mounted on top is displayed. Human operators at dedicated workstations are alerted in order to validate

50 a fire and, if validated, they notify fire protection agencies in order to initiate firefighting efforts (Heyns  
51 et al., 2019).



52  
53

54 Figure 1 (a) Camera used in a CWDS; (b) a 32-m tower on top of which a camera is placed, with the solar power supply visible  
55 near the base of the tower (Heyns et al., 2019).

56 The process of configuring the sites at which the towers of a CWDS are placed is critical to overall system  
57 detection potential with respect to the surrounding environment. Historically, site locations for CWDSs  
58 (or, more traditionally, watchtowers) have been planned without the use of computational optimisation  
59 tools by foresters and locals with intimate knowledge of the terrain. The areas that are considered to offer  
60 good candidate tower sites can be large and envelop expansive terrain surfaces (Heyns et al., 2019). The  
61 selection of a number of specific site locations – corresponding to the number of towers available –  
62 located on these large terrain surfaces poses a significant challenge. Simply identifying individual sites  
63 with good visibility cover of the surrounding environment would result in a number of cameras with good  
64 individual visibility. This is not a desired approach for *system* optimisation, where the overall detection  
65 potential depends on the *combined* visibility cover of *all* the cameras in the system instead of individual  
66 camera coverage.

67 When entering unfamiliar territories, the knowledge and expertise of foresters and locals may not be  
68 available to system planners. Selecting multiple tower sites to achieve comprehensive coverage becomes  
69 an even more daunting challenge in such instances. This can be alleviated by considering various  
70 combinatorial optimisation solution approaches which exist to identify multiple observation points with  
71 the aim of maximising *system* coverage – for examples, see (Bao et al., 2015), (Tong et al., 2009), (Zhang  
72 et al., 2019) and (Kim et al., 2004). The problem with relevant approaches from the literature, however,  
73 is that they are theoretical and do not address the *real-world* challenges associated with site selection  
74 problems. For example, these studies involve unrealistically small, square-shaped study areas with  
75 hypothetical test scenarios – and have no existing systems available in their study areas to at least provide  
76 some benchmark for their solution frameworks. Tower site selection approaches destined for large and  
77 more practically realistic areas exist (Eugenio et al., 2016), but are aimed at maximising single-site  
78 visibility cover with the potential for good system cover, rather than explicitly pursuing system coverage.  
79 A comprehensive framework aimed at the optimisation of *system* coverage achieved by CWDSs over  
80 *large* prescribed regions therefore remains absent from the literature.

81 To address the practical limitations from the literature, an optimisation framework for CWDSs has been  
82 under development with collaboration from *ForestWatch* (evsusa.biz) – a South African-developed  
83 CWDS with extensive operations in various critical regions in South Africa, and worldwide. The camera  
84 and tower in Figure 1 are, in fact, part of a ForestWatch CWDS in South Africa. Guided by their feedback  
85 and experience from an operational point of view and with the aim of maximising CWDS coverage, the  
86 intended purpose of this framework has evolved to a) determine multiple candidate CWDS tower-site  
87 layouts, b) within short timeframes (less than a week), and c) with minimal user input. Initial development  
88 of the framework investigated the wildfire-prone, mountainous region of Nelspruit in South Africa in  
89 which an existing twenty-tower CWDS served as a benchmark. The effectiveness of this benchmark  
90 CWDS has been proven by its daily detection numbers – in 2017 alone, the system logged 2786 alerts  
91 within the subscribed client area, and many more outside (Heyns et al., 2019). The smoke detection  
92 potential of the existing layout was compared to that which could be achieved by solutions determined  
93 by heuristic optimisation, and heuristic-obtained solutions outperformed the existing system (Heyns et  
94 al., 2019). Having such a successful existing system available as a benchmark for comparison together  
95 with guidance from technical experts from the region (who selected the sites for the existing system)  
96 allowed us to develop our approach with a level of detail and practical inspection which is missing from  
97 related studies in the literature. The study was expanded by investigation into the implementation of  
98 landform-based site selection (e.g. peaks, ridges, slopes) to improve our candidate site selection process  
99 (Heyns et al., 2020). The results allowed us to consider additional solution approaches which led to  
100 improved results within reduced computation times compared to our first attempts from Heyns et al.  
101 (2019). The problems above illustrated how using geographical information systems (GIS) together with  
102 our *multi-objective* (MO) optimisation approaches could drastically improve future CWDS system  
103 planning – not only in coverage maximisation but also in easing the actual decision-making processes.

104  
105 The focus of this paper is to present two recent real-world tower site-selection problems that implement  
106 and build on the previous framework development (Heyns et al., 2019, 2020). First, a search for  
107 alternatives to thirteen separate towers proposed by ForestWatch technicians in the Mpumalanga province  
108 was investigated. This presented us with an opportunity to develop and implement a novel single-site  
109 selection framework for the identification of alternative sites for *individual* towers, as opposed to *system-*  
110 *tower* optimisation which had been the previous research focus. Single-site search approaches are not  
111 uncommon in the literature (Tabik et al., 2013; Zhang et al., 2019); however, approaches to search for  
112 *alternatives* for proposed sites do not exist. This also provided the first opportunity for practical  
113 implementation of landform-based site selection. The framework identified numerous alternatives for  
114 each of the thirteen sites proposed by ForestWatch, and six alternatives were eventually chosen above  
115 expert-selected sites. Furthermore, the single-site selection framework introduced new coverage  
116 evaluation criteria which had not been investigated in our previous work, nor in the related literature.  
117 These new coverage criteria are poised for consideration as additional objectives in future  
118 implementations of our framework.

119  
120 Moving on from the single-site selection problem, the system-optimisation framework was showcased as  
121 fully-functioning and practical when it was applied to select sites for a new four-tower CWDS in South  
122 Africa’s Southern Cape. Rural villages are found in this region and many of the local population are  
123 employed by the forestry sector. In 2017, in the town of Knysna (a mere 60 km away), one of South  
124 Africa’s most devastating fires ever occurred (Forsythe et al., 2019). The study area exhibits similar  
125 vegetation and terrain to the Knysna area – a similar catastrophe occurring is thus a very real possibility  
126 and was one of the driving factors for the decision to install a CWDS here. Rapidly-determined layouts  
127 from our framework drastically outperformed the coverage achieved by sites initially proposed by  
128 technical experts with years of experience in forestry and tower site selection (and which required weeks  
129 of planning). One of our solutions was eventually selected instead of their initial layout, although two of  
130 its four tower sites were slightly altered by the decision-makers for practical purposes which are  
131 elucidated later. ForestWatch requested alternative layouts days before a contract proposal deadline – the  
132 fact that numerous superior and practically implementable layouts were obtained within such a short  
133 timeframe further substantiates why ForestWatch plans to implement the framework in future site-  
134 selection problems. Collaboration with decision-makers in determining tower sites before and after  
135 computational optimisation revealed interesting practical considerations and important guidelines for

136 future work – a novel contribution to the literature related to similar problems in which the focus is  
137 overwhelmingly theoretical.

138  
139 The paper opens with a summary of CWDSs in terms of their detection requirements and the factors that  
140 need to be considered in the planning of their tower site locations. The GIS component of our framework  
141 is elucidated, which includes a review of candidate site selection methods and how GIS is used in our  
142 framework for this purpose. Processes for the selection of final tower sites are then described, specifically  
143 related to optimisation methods and those implemented within our framework. The two problems  
144 presented in this paper are then discussed in terms of the project requirements and the data and methods  
145 used. The results are then presented, followed by a discussion and a brief conclusion.

## 146 2 Background

### 147 2.1 Camera-based wildfire detection systems

148 The type of clients that subscribe to CWDSs vary regionally. In South Africa they are forestry companies,  
149 while in the USA and Canada they are either local or federal government agencies. Subscription cost  
150 models vary between CWDS service providers. Some providers charge fixed fees per tower, while a  
151 provider such as ForestWatch calculates a subscription fee in relation to the total client-area coverage  
152 achieved. Coverage maximisation therefore not only contributes towards a CWDS’s ability to detect  
153 smoke and initiate a response but may also result in increased subscription revenue. The client typically  
154 pays for the tower and equipment installation costs, providing further motivation to achieve  
155 comprehensive visibility coverage with the minimum number of required towers. Minimising the number  
156 of required towers to achieve optimal cover also results in reduced future expenses on maintenance and  
157 upgrades.

158  
159 ForestWatch CWDSs detect smoke patterns and their effectiveness depends on their ability to observe  
160 smoke above the terrain surface (Heyns et al., 2019; Hough, 2007; Schroeder, 2005) – their algorithm is  
161 based on automated detection of aurora which they developed in Antarctica (Hough, 2007). This differs  
162 from the standard approach followed in surveillance system applications (including those related to  
163 CWDSs), where visibility is evaluated with respect to the terrain surface (Bao et al., 2015; Franklin, 2002;  
164 Kim et al., 2004; Tabik et al., 2013). In order to be visible from a camera, smoke needs to rise from the  
165 ground and typically needs to clear visibility obstruction from terrain and vegetation. Once smoke is  
166 identified, human operators are alerted and detection reports are sent. Detecting a smoke plume as low  
167 as possible above the terrain surface allows more rapid suppressing action to be taken after the onset of  
168 the fire. However, a camera's visibility of smoke is more likely to be obstructed by terrain and vegetation  
169 when the smoke is near the terrain surface or the fire is in a valley or behind a hill, as shown in Figure 2.  
170 A CWDS’s overall detection potential therefore also depends on its ability to detect smoke at higher levels  
171 above the terrain surface (after clearing obstructions). Furthermore, CWDSs may be configured in such  
172 a manner that they achieve satisfactory visibility cover over *buffer zones* (Heyns et al., 2019). Buffer  
173 zones extend beyond the client boundaries since external fires may well encroach onto the client area and  
174 are also crucial to monitor.

175

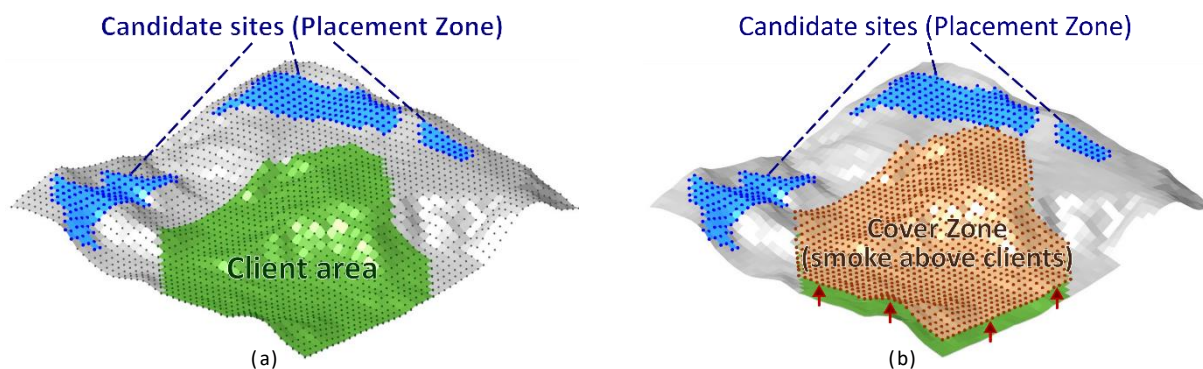


176

Figure 2 Wildfire detected by the ForestWatch CWDS, displaying typical visibility obstruction caused by terrain.

177 **2.2 Terrain and candidate site representation**

178 CWDS site-selection optimisation requires an appropriate data environment within which to function.  
179 Raster data is employed extensively in the literature for solving facility location problems similar to the  
180 CWDS site-selection problem (Franklin, 2002; Heyns and Van Vuuren, 2018; Kim et al., 2004; Kwong  
181 et al., 2014) and represent the earth's surface and environmental information as uniformly spaced sample  
182 points across the terrain. A raster data representation of a hypothetical terrain surface is provided in  
183 Figure 3(a). The non-contiguous blue surface area is an example of suitable terrain identified for the  
184 placement of towers – subject to factors such as allowable geographical and administrative/municipal  
185 boundaries, and suitable terrain characteristics, or manual selection. The green surface area is an example  
186 of an area that requires monitoring and, in the context of this paper, is land belonging to forestry clients.  
187 The dots on the terrain surface are uniformly spaced satellite-sampled elevation data, which are used to  
188 generate the surface. The distance between neighbouring sample points is approximately 30 m at the  
189 highest resolution of raster data that is publicly available. The sites that may be considered for facility  
190 placement (the blue dots) collectively form the Placement Zone (PZ).  
191



192 (a) (b)  
193 Figure 3 Raster data represent the earth's surface as uniformly spaced sample points (Heyns et al., 2019). (a) Raster representation  
194 of a terrain surface with a PZ and client area; (b) raster representation of a Cover Zone above the client area.

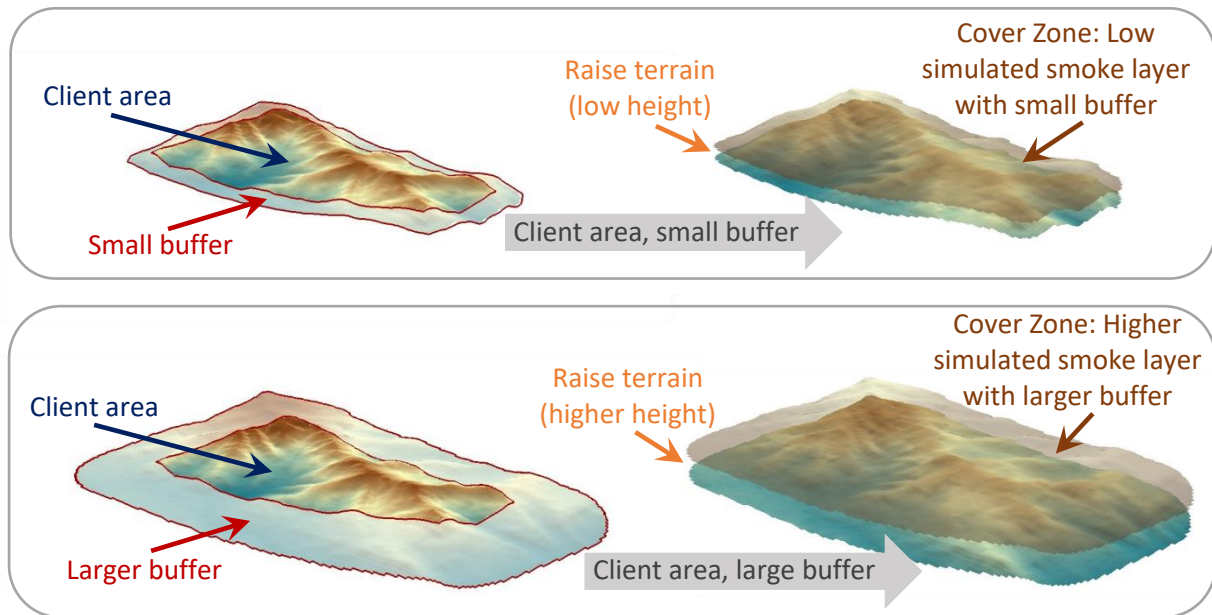
195 **2.3 Smoke layers and buffers**

196 Detection potential is evaluated according to coverage achieved with respect to areas known as *Cover*  
197 *Zones (CZs)*. In the context of CWDSs, a CZ is simply the rasterised terrain surface that falls within the  
198 client area (and extended to within some buffer boundary) raised to a specified height above the ground  
199 (simulating a layer of smoke) so that the system's potential for detecting smoke at that height may be  
200 evaluated. The buffer zone added to the smoke layer allows monitoring of the progress of fires outside  
201 the client area – these fires need to be monitored by ForestWatch, but client response is not necessarily  
202 required if their properties are not under immediate threat. An example of a CZ is illustrated in Figure  
203 3(b) – the brown surface and markers above the client area.  
204

205 In our framework, the CZs are considered at different heights above the terrain surface. One of the main  
206 added advantages of using more than one smoke height and buffer distance is that different tower-site  
207 combinations which contain sites at different locations are typically found to provide superior detection  
208 potential with respect to each CZ (Heyns et al., 2019). This leads to more diverse solutions and trade-off  
209 alternatives for decision-makers, i.e. more options (the benefits of this in the practical decision-making  
210 process are discussed in more detail later). Smaller buffer zones (0 to 500 m) are added to lower layers,  
211 intended for near-immediate detection and rapid response. The detection potential of higher layers gauges  
212 how well the system can detect smoke that has risen from the lower layers to clear obstructions to  
213 (potentially) be visible. Extended buffer zones (500 m to 4 km) are added to these higher layers. Figure  
214 4 provides a visual description of the GIS processes involved in generating CZs using these methods.  
215

216 The portion of a CZ that is visible from a camera is referred to as its *viewshed*, and is computed from a  
217 collection of line-of-sight queries between the camera and all the demand points within the CZ, limited  
218 by terrain interference and the camera's detection range (Kim et al., 2004; Nagy, 1994). A system

219 viewshed of a CZ is then the merged viewsheds of all the individual cameras in the CWDS with respect  
220 to the CZ – i.e. the demand points in the CZ that are visible from at least one camera in the system.  
221  
222



226 Figure 4 Buffers zones are added around the client area to monitor threatening external fires, and the combined client and  
227 buffer terrains are raised in order to simulate smoke layers at different heights above the terrain surface (the CZs). A small  
228 buffer with a low height is used to determine a CWDS’s near-immediate detection capability (top image), while a larger buffer  
229 with a higher height is used to evaluate secondary detection potential (bottom image).

## 230 2.4 Candidate site identification

231 Identifying the candidate sites from which final tower sites are selected is a sensitive process. From an  
232 initial, “rough” pool of candidates, weaker sites may be identified and discarded, resulting in a stronger  
233 pool of candidates – while simultaneously reducing the computational complexity of the problem (Heyns  
234 et al., 2020). Caution should, however, be taken to avoid the possibility of removing good candidate sites  
235 by untested or excessive reduction techniques. Our approach requires the identification of candidate sites  
236 for single- and system-site searches, for which approaches have been described in the literature.  
237

238 The least sophisticated candidate site selection approach is also the most arduous and time-consuming,  
239 namely manual candidate site selection. This approach is only relevant in small, hypothetical problem  
240 areas in which manual terrain inspection is a viable approach. Examples in the context of wildfire  
241 detection include the selection of 34 candidate sites by Zhang et al. (2019) and 30 candidate sites by Bao  
242 et al. (2015) – both study areas were smaller than 11 sq. km. and rectangular due to the theoretical focus  
243 of their work. The average ForestWatch system covers a surface area of well over 200 sq. km, and the  
244 practical implementation later in this paper has a client area of approximately 435 sq. km. These  
245 expansive terrains typically contain numerous mountains, hills and ridges, so manually identifying  
246 candidate sites would become impractical. This does not mean that manual site selection is impossible  
247 in such large areas – the existing towers in large regions monitored by ForestWatch have been selected  
248 manually. However, this has only been possible because technicians and experts with decades of  
249 experience in the regions were familiar with the terrain and because of historical lookouts and existing  
250 infrastructure in the areas already being well known. Even then, the manual site selection and inspection  
251 process took months (Heyns et al. 2019) and moving into unfamiliar terrain would pose an even greater  
252 challenge. Manual site selection is therefore not suitable for our purposes.  
253

254 GIS approaches offer a relatively simple alternative and is suitable for identifying candidate sites in  
255 significantly large areas, while ensuring that the sites are practically feasible. Eugenio et al. (2016)  
256 searched for sites for manned watchtowers in a large area covering 46 000 sq. km in Brazil. GIS analyses  
257 were first used to identify land within feasible geographical and administrative/municipal boundaries,

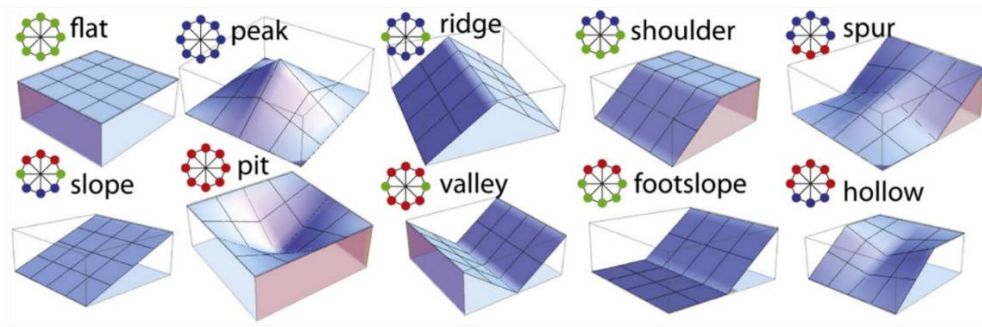
258 after which terrain feature classification analyses were used to identify ridges on mountains and hills.  
259 Areas on the terrain that were within suitable distances from roads were also identified. Sites that fell  
260 within a feasible terrain surface that satisfied all three criteria of feasible land, ridge features, and suitable  
261 road access resulted in a final set of candidates which were considered for watchtower placement. This  
262 method of site identification avoids the manual process followed by Bao et al. (2015) and Zhang et al.  
263 (2019) and is suitable for implementation in our approach. We use similar GIS approaches to those used  
264 by Eugenio et al. (2016) to identify suitable areas from which candidate sites may be selected (Heyns et  
265 al., 2019), discussed next. The disadvantage of the approach is that it results in unusually large numbers  
266 of candidate sites, but this is mitigated using combined heuristic approaches in our framework.

## 267 2.5 GIS for candidate site selection

268 The GIS component of our framework limits the terrain that lies within client boundaries to raster points  
269 which exhibit suitable characteristics for tower placement. First, terrain with a degree of slope over 12°  
270 (or 20%) should be avoided to ensure that tower installation may be performed without the need for  
271 excessive terrain alteration, in addition to ease of access on foot. Second, for transportation and general  
272 access purposes (*e.g.* construction and maintenance), a distance of 100 m or less to roads is deemed  
273 necessary. The criterion of proximity to power supplies has been considered, but solar power supplies  
274 are generally installed due to an inconsistent power supply system in the South Africa and theft (a solar  
275 power supply can be seen in Figure 1(b)). Nevertheless, access to power may yet be implemented in  
276 future problems – its (indirect) importance in practice was illustrated in the decision-making process of  
277 experts related to the problems presented in this paper. Software such as the commercially available  
278 ArcGIS 10.5.1 can be used for the purpose of terrain and site analysis. Feasible slope sites are determined  
279 with 30 m resolution raster elevation data and the ArcGIS slope tool, while road-accessible sites are  
280 determined with roads data obtained from the clients in the study area and the ArcGIS Euclidean distance  
281 analysis tool. The resulting PZ consists of sites which satisfy both these requirements. These criteria and  
282 analyses were shown to be realistic when it was found that the sites of 26 towers in the benchmark  
283 Nelspruit CWDS were all located at sites which satisfied these requirements (Heyns et al., 2019).

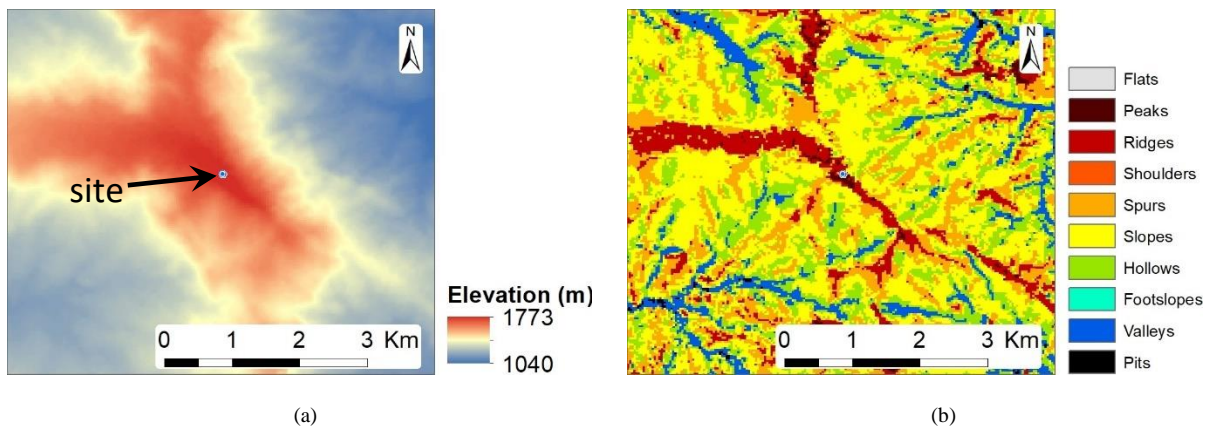
284  
285 Reducing the size of the PZ to landforms that are typically associated with superior visibility – more  
286 generally referred to as the *reduced observer strategy* (Rana, 2003) – is also integrated in our framework  
287 (Heyns et al., 2020). In the related literature, ridges and peaks are consistently considered to offer superior  
288 observer visibility compared to sites classified otherwise (Franklin and Clark, 1994; Kim et al., 2004;  
289 Lee, 1994; Rana, 2003). Reducing the PZ to such landform types reduces the number of candidate sites  
290 and results in reduced combinatorial complexity, while it has also been shown that the approach results  
291 in improved solution quality because superior sites are considered in the search process and inferior ones  
292 are avoided. Our framework implements *geomorphons* – these are pre-defined terrain patterns that are  
293 matched to land surfaces according to similarities in their geometry (Jasiewicz and Stepinski, 2013). In  
294 a single, simple execution (requiring a single line of code) the geomorphon tool can identify ten  
295 significant landform classes: flats, peaks, ridges, shoulders, spurs, slopes, pits, valleys, footslopes and  
296 hollows, as illustrated in Figure 5. The geomorphon classification approach is implemented in our  
297 framework due to its simplicity and availability in open-source software, and its proven practicality in a  
298 variety of recent problems (Di Stefano and Mayer, 2018; Djurdjevac Conrad et al., 2018; Harmon et al.,  
299 2018; Luo and Liu, 2018). All geomorphon classifications in this article were processed in the GRASS  
300 7.4.0 software environment. An example of the results of a geomorphon classification is provided in  
301 Figure 6 for the terrain surrounding a tower site in (a), with the corresponding geomorphons in (b).

302



303  
304  
305  
306

Figure 5 Terrain landform classifications of (Jasiewicz and Stepinski, 2013). The colours of the patterns alongside each class indicate differences in elevation with respect to the centre point – green indicates same height, red indicates higher, blue indicates lower.



307  
308

Figure 6 (a) Terrain elevation around a proposed site location, and (b) the corresponding geomorphon landform classification of the surrounding terrain.

311 The strategy of selecting candidate sites according to landforms such as peaks and ridges should, however,  
 312 be approached with caution because a level of uncertainty is introduced which may result in good sites  
 313 being discarded (Romero and Clarke, 2018). Therefore, to avoid the unsubstantiated implementation of  
 314 geomorphons it was decided to first analyse the terrain feature classes at 165 ForestWatch towers from  
 315 systems in Mpumalanga Province in South Africa (93 towers), Douglas County in the state of Oregon,  
 316 USA (31 towers) and the central region of Saskatchewan Province in Canada (41 towers). This was the  
 317 first time that such a *practical* site classification exercise has been performed for *existing* facilities, as  
 318 opposed to some traditional analyses in a theoretical context related to terrain only – e.g. those performed  
 319 by Kim et al. (2004) and Rana (2003). It was found that 136 (or 82%) of the towers were sited at peak or  
 320 ridge sites as classified by the geomorphon approach, while those that are sited otherwise are never far  
 321 away from peaks or ridges (less than 175 m) (Heyns et al., 2020). Discussions with ForestWatch  
 322 technicians revealed that some towers are located at sites classified other than peaks or ridges because  
 323 even though the peak or ridge sites would actually be preferred, they are sacrificed for nearby alternatives  
 324 due to factors such as ground condition and accessibility. Nevertheless, peaks and ridges are the go-to  
 325 sites according to geomorphon landform analysis and according to technicians. Identifying candidate  
 326 sites that are limited to peaks and ridges should therefore provide decision makers with sites that are either  
 327 a) practical and selected for final implementation, or b) sufficiently close to nearby alternatives which  
 328 may be considered more suitable for practical reasons.

## 329 2.6 Final tower site selection

### 330 2.6.1 Practical processes

331 In practice, the selection of final tower sites is an iterative process between CWDS providers and clients  
 332 and/or detection agencies involved in protecting a specific region, and will often aim to finalise and  
 333 deploy a CWDS layout in time for a fire season. In the past, this lengthy process (without significant use  
 334 of any computerised support) has led to suitable strategies not being agreed upon in time for a CWDS's



335 deployment prior to a fire season, resulting in the deployment being delayed another year and the  
336 vulnerable region being left to endure one more season with existing, outdated and inferior detection  
337 ability – or none at all. When determining a suitable CWDS layout, the client should be pleased with the  
338 predicted detection coverage, while the cost of the installation and operation of towers is also important.  
339 The towers are generally sited on the client’s property and the client may dislike one or more sites for  
340 subjective reasons. Such scenarios require technicians to conduct the site-selection process anew, with  
341 the possible requirement of finding alternatives for *all* the proposed sites (i.e. no sites retained). This is  
342 because moving a single undesirable site not only influences its individual coverage, but that of the system  
343 – resulting in its relocation requiring the relocation of another tower to compensate for the changes in  
344 system coverage, followed by further relocations to offset the second relocation’s effects, and so on.  
345 Naturally, reducing the number of towers required to achieve satisfactory cover is preferred, to reduce  
346 installation and operational costs, and to reduce the physical client property required for installation.

347  
348 Due to factors such as those mentioned above, decision-makers would benefit from obtaining *multiple*  
349 CWDS layout alternatives from a decision-support framework. They may browse through proposed  
350 coverage maps achieved by these layouts and identify those which they consider to offer the best client  
351 coverage. The tower locations of their preferred layouts may then be investigated – this may be performed  
352 virtually with tools like Google Earth to perform a basic assessment, followed by physical site inspections  
353 if necessary. In the event that the client dislikes one or more sites in a preferred layout, alternatives which  
354 do not include the undesirable sites may be investigated. Furthermore, if specific sites that are considered  
355 undesirable by the client appear in multiple preferred layout proposals, it should be possible to remove  
356 them from consideration and *rapidly* repeat the optimisation process anew, providing new coverage maps  
357 achieved with more suitable CWDS layouts. Our framework has been developed with these key  
358 requirements in mind.

359 After the final tower sites have been agreed upon, a suitable tower height at each site needs to be  
360 determined. Extensions to base tower heights are normally added because an increase in tower height  
361 improves overall smoke detection potential by allowing a camera to see over obstructions. Base structures  
362 typically stand 12 m tall in South African projects and height increases are achieved by adding one or  
363 more extensions to these, normally in 3 m increments (Heyns et al. 2019). An increase in tower height at  
364 a site depends on a) whether an increase in tower height is required for the camera to rise above the  
365 canopy of surrounding trees, b) the actual need for an increase in height from the base, depending on  
366 client coverage already achieved from the base height, and c) whether the demands of an increase in  
367 structure size and support (in terms of the tower foundation and stabilisation wires that increase in span  
368 as tower height increases) can be accommodated at the site. For the remainder of this paper, it is assumed  
369 that site searches are performed with 12-m towers only and the focus is on site-selection only.  
370 Furthermore, a camera range of 8 km is generally used by ForestWatch for site search analyses in South  
371 Africa and will also be used for site search analyses in this paper (the cameras have a visible range of  
372 well beyond 8 km, but 8 km is used for contractual purposes).

### 373 2.6.2 *Computational methods*

374 Theoretical research into the evaluation of multiple candidate viewpoints’ viewsheds from which a  
375 superior site may be identified is available in the literature (Lee, 1994; O’Sullivan and Turner, 2001;  
376 Tabik et al., 2013). Such computational approaches provide a platform for *single-site* searches. Zhang  
377 et al. (2019) perform sequential single-site searches after determining their 36 candidate sites for wildfire  
378 detection purposes. First, the viewsheds and covering percentages of each candidate site is determined  
379 and the single site with the best coverage is selected for tower placement. The selected site is removed  
380 from the set of candidates, the demand region is updated by removal of the demand area covered by the  
381 new tower, and then the next tower site is determined by finding the next candidate site with the best  
382 coverage over the updated demand. This process is then repeated until a budget limit has been reached,  
383 or until acceptable cover has been determined. While this final site-selection process is more user-friendly  
384 than a manual approach, it is a repeated single-site search destined for incremental expansions to existing  
385 towers – the process is not aimed at system-optimisation. This approach is therefore not considered  
386 suitable for our requirements, but an approach similar to their sequential one was implemented in our  
387 single-site alternative searches. However, compared to the literature in which a superior site is sought

388 based on the coverage determined with respect to the surrounding terrain surface, our requirements are  
389 unique. Instead, we search for the best *alternatives* within a local proximity to an already proposed site  
390 – a requirement not previously considered in the literature. Furthermore, we evaluate alternatives  
391 according to three covering objectives in our single-site alternative search – resulting in more than one  
392 alternative – whereas the related literature focusses on identifying the single point with the best visibility  
393 according to a single covering criterion.

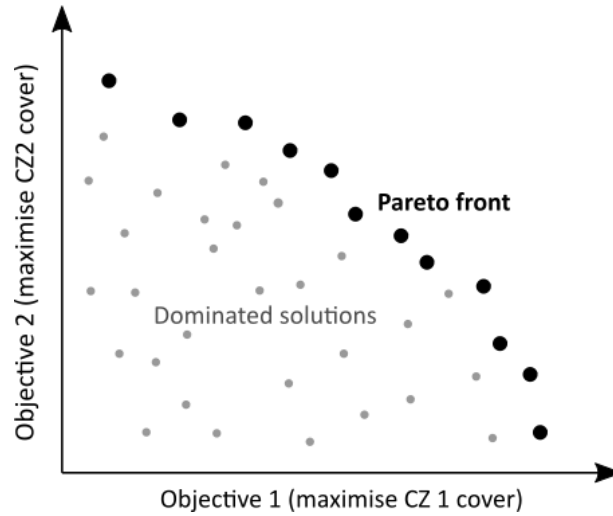
394  
395 Eugenio et al. (2016) followed an interesting approach which essentially combines multiple localised  
396 single-site searches for overall system-optimisation. Their 46 000 sq. km study area was sub-divided into  
397 uniform square cells with the sides measuring 15 km, 17.5 km, and 20 km in separate analyses. The site  
398 with the highest altitude within each cell was selected as a watchtower site (constrained to suitable land  
399 boundaries, ridge features, and road access). In this manner, they were able to rapidly determine over 130  
400 towers at a time in separate analyses, with the assumption that each tower in each cell would provide a  
401 good contribution to the overall system coverage of all the towers combined. The disadvantage of the  
402 approach is that the final selection of sites is limited to a single one within each cell and is ultimately  
403 based upon altitude. As is the case with manual site selection, merely identifying multiple sites which  
404 may provide individual watchtowers with good visibility does not guarantee good overall system cover.  
405 Their approach does not consider overall system coverage in the site selection process, and system  
406 coverage is only determined post-site selection. The approach may also result that superior system-sites  
407 are discarded within a cell because of it not providing the best perceived individual cover in the cell.  
408 Furthermore, high altitude alone does not necessarily ensure good visibility from a site and its relationship  
409 with its surrounding environment, and towers, is equally important (Franklin and Clark, 1994; Misthos et  
410 al., 2018) – especially when the aim is system coverage optimisation. This process is therefore not  
411 considered for our framework.

412  
413 Bao et al. (2015) investigated the use of integer-linear programming and a genetic algorithm for “true”  
414 *system-optimisation*. They obtained candidate CWDS layouts comprising between six and sixteen  
415 watchtowers in single runs selected from thirty candidate sites – determined specifically with respect to a  
416 system coverage maximisation objective. While their theoretical study was conducted in an impractically  
417 small area of 10 sq. km and their sites were manually selected, the computational approaches that they  
418 followed are perfectly suited to our framework. Our problems, however, require additional heuristic  
419 approaches as a result of our significantly large, real-world territories and the resulting computational  
420 complexity. These approaches are discussed next.

## 421 2.7 Optimisation of tower site selection

### 422 *2.7.1 Pareto-optimal solutions*

423 Our objectives are to maximise the percentage of points in each CZ which are visible, i.e. to maximise  
424 visibility with respect to different smoke layers. Candidate CWDS layouts are evaluated by objective  
425 functions which calculate their detection potential with respect to each CZ. This translates to a single  
426 point in *objective function space* for each candidate layout (i.e. candidate solution), as is illustrated in  
427 Figure 7 in which a number of candidate layouts have been evaluated. The example in Figure 7 considers  
428 two CZs, which correspond to the two objectives on the axes, but the same principles apply for three or  
429 more objectives.  
430



431

432 Figure 7 The notions of solution domination and of a Pareto front in objective function space.

433 In MO optimisation, solutions such as those in the figure are classified either as *non-dominated* (superior)  
 434 or *dominated* (inferior) solutions (Zitzler et al., 2004). Dominated solutions are avoided, since for each  
 435 dominated solution there exists at least one non-dominated solution that is equally good with respect to  
 436 all the objectives, and is better in at least one. Amongst the solutions in the non-dominated set, each  
 437 solution outperforms another in at least one of the objectives while simultaneously being weaker in at  
 438 least one of the others. The set of non-dominated solutions exhibit superior trade-off alternatives to the  
 439 dominated solutions, and form what is commonly known as the *Pareto-optimal front*, or simply the *Pareto*  
 440 *front*, as may be observed in Figure 7 (Zitzler et al., 2004). Only the solutions on the Pareto front need to  
 441 be presented to decision makers because of their superior quality.

### 442 2.7.2 Stage 1 - heuristics

443 The set of all possible solutions to a problem, *i.e.* all the possible candidate CWDS layouts on the terrain,  
 444 is called the *solution space*. If  $N_t$  and  $N_s$  denote the number of towers available for placement and the  
 445 number of feasible sites, respectively, the number of possible solutions,  $N_p$ , is

446

447

$$N_p = \binom{N_s}{N_t} = \frac{N_s!}{N_t!(N_s - N_t)!} \quad (1)$$

448

449 The number  $N_p$  is imposingly large in problems such as those investigated in this paper, because the large  
 450 scale of territories in which ForestWatch operate and the choice of a GIS-based candidate site  
 451 identification approach. The pursuit of the *exact* (true) Pareto front in such instances (and in other MO  
 452 facility location problems that include covering objectives) involves a significant computational challenge  
 453 and become prohibitively large to solve within realistic computation times (Jia et al., 2007; Owen and  
 454 Daskin, 1998; ReVelle and Eiselt, 2005; Tong et al., 2009; Xiao et al., 2002). Furthermore, not only is  
 455 the search combinatorially complex in terms of the number of candidate sites and towers to place, but the  
 456 computation of viewsheds (and system-viewsheds) in visibility-cover location problems imposes an  
 457 additional and time-consuming computational burden (Heyns and van Vuuren, 2016).

458 In instances such as these, powerful heuristics are often employed in order to *approximate* the set of  
 459 solutions on the Pareto front within realistic computation times (Bao et al., 2015, Xiao et al., 2002; Zitzler  
 460 et al., 2004). These heuristics explore promising regions of the solution space in order to determine  
 461 solutions that are approximately Pareto-optimal, and in the process avoids the computationally expensive  
 462 consideration of solutions in inferior regions of the solution space. It has been demonstrated in the  
 463 literature that heuristics are well capable of determining the true Pareto front (Heyns and Van Vuuren,

2018; Heyns and van Vuuren, 2016; Kim et al., 2008). *Multi-Objective Evolutionary Algorithms* (MOEAs) are able to approximate a diverse set of trade-off solutions on the Pareto front in a single run (Fonseca and Fleming, 1993; Purshouse and Fleming, 2003) and are also known to achieve good results fast (Alp et al., 2003). Examples of the application of MOEAs to solve problems similar to CWDS planning include the placement of transmitters (Meunier et al., 2000; Raisanen and Whitaker, 2005), wind turbines (Kwong et al., 2014; Yamani Douzi Sorkhabi et al., 2016), and observation equipment (Bao et al., 2015; Heyns and Van Vuuren, 2015; Kim et al., 2004; Tong et al., 2009). However, when a problem is sufficiently large and the location of the true Pareto front is unknown, there is no guarantee that the obtained solutions are on or even near to the true Pareto front.

The *non-dominated sorting genetic algorithm-II* (NSGA-II) is a popular MOEA that is classified as a *genetic algorithm*, in which a candidate CWDS layout is represented as a *chromosome* string of  $N_t$  feasible tower site numbers (Deb et al., 2002; Heyns et al., 2019). Site numbers are indexed for all the sites within the PZ's raster representation – typically derived with respect to row and column indices (Heyns and van Vuuren, 2016). For example, a chromosome [22, 115, 698, 739] represents a candidate CWDS with four towers located at sites 22, 115, 698 and 739. Evolution-inspired selection processes and modification operators are iteratively performed on a randomly generated population of such candidate CWDS chromosomes. The process is repeated until some termination criterion is met (Deb et al., 2002). One typical termination criterion is when successive populations fail to significantly improve on the solution quality of previous generations (Heyns, 2016). More detailed descriptions of the NSGA-II as used for our purposes are available in the literature (Heyns et al., 2019; Heyns and van Vuuren, 2016).

The large scale of territories in which ForestWatch operate and the implementation of a GIS-based candidate site selection approach instead of a manual one leads to a large number of candidate sites to consider in our problems – especially when compared to similar site optimisation problems in the literature (Bao et al., 2015; Kim et al., 2008, 2004; Tanergüçlü et al., 2012). The addition of viewshed-based covering objectives further adds to this computational complexity. Unique to our framework is the implementation of our *multi-resolution approach* (MRA) (Heyns, 2016; Heyns and van Vuuren, 2016) which alleviates this computational burden. The MRA is a recent, novel optimisation tool that was specifically developed for geospatial facility location problems with unusually large solution spaces such as those faced by ForestWatch. It has been shown that implementation of the MRA results in little or no reduction in solution quality, and in some instances can even lead to improved solution quality within drastically reduced computation times (Heyns, 2016; Heyns and van Vuuren, 2016).

The MRA simplifies the site search by first determining candidate layouts using a low-resolution grid of the candidate sites extracted from the high-resolution ones included in the feasible PZ area – effectively reducing the number of candidate sites. The NSGA-II is then run to approximate the Pareto front using this low-resolution PZ. The sites that are included in the solutions from this low-resolution Pareto front approximation are considered to be indicative of local regions which contribute favourably to optimal system coverage and merit further exploration. Thus, a finer resolution is used to intensify the search in the regions around these sites with additional optimisation runs. This is achieved by taking the low-resolution Pareto-front sites together with their high-resolution local neighbours, and pooling them together into a high-resolution pool of candidate sites – i.e. a new PZ.

Two resolutions have been used in our framework development (Heyns et al., 2019, 2020) and the real-world CWDS optimisation problem presented later in this paper. The first, lower resolution uses a spacing of approximately 90 m between neighbouring sites in the PZ (from the initial, higher resolution 30-m spacings). Then, around all the sites in the low-resolution Pareto front approximation, the feasible sites within a 5×5 raster-point neighbourhood at spacings of 30 m are selected and included in the high-resolution PZ. The algorithm is then run again with consideration of this high-resolution PZ. As an example of the initial reduction in computational complexity that may be achieved, the number of feasible sites in the PZ from our first study was reduced from 741 813 at 30-m spacings down to 82 547 at 90-m spacings (Heyns et al. 2019). The MRA also reduces the number of required viewshed computations and their associated computation time requirements, because the search is limited to promising regions and weaker ones are avoided (Heyns and van Vuuren, 2016). Most importantly, the MRA identifies and

517 focuses on regions which contain sites that contribute to good overall *system* cover and not just on  
518 individual sites with good visibility.

### 519 2.7.3 Stage 2 - additional optimisation

520 The first optimisation stage as described above entails using the MRA-NSGA-II at two resolutions to  
521 determine multiple CWDS layouts. The final candidate layouts include multiple strong sites, but the  
522 unusually large size of our solution space and the approximation characteristics of the heuristic approach  
523 still do not guarantee that the solutions are optimal or even near-optimal. We therefore perform an  
524 additional optimisation stage.

525 The additional optimisation stage does not focus on determining new, alternative sites to those obtained  
526 in the first stage, but instead focusses on searching for improved site-combinations of these sites. These  
527 strong sites included in the Pareto-front approximations from the first stage are pooled together into a new  
528 PZ. This relatively small post-heuristic PZ then serves as input into the second stage's optimisation  
529 process in which additional runs can be performed – using either heuristics or ILP – without  
530 implementation of the MRA. Using the NSGA-II during this additional stage has been shown to result in  
531 significant improvement in the solution quality of CWDSs (Heyns et al., 2019). The number of sites in  
532 the new PZ is typically such a comparatively small number (compared to the size of the original PZs) that  
533 it has also introduced the possibility to implement an ILP weighted-sum approach as an alternative to  
534 heuristics in the second stage (Heyns et al., 2020). An ILP approach had not been considered previously,  
535 because ILP solver software are sensitive to the size and complexity of the problems which they can solve  
536 – heuristics, on the other hand, can attempt to find solutions to any size problem.

537 Commercial ILP software packages (e.g. CPLEX and Gurobi) take as input an ILP formulation of an  
538 objective function and constraints and return a single solution. Once the problem becomes multi-  
539 objective, the objectives are often weighted and summed together into a single objective function in order  
540 to satisfy the single-objective limitation of these software packages (Cohon, 1978; Murray et al., 2007).  
541 An approximation to the Pareto front is traced out by varying objective weights in multiple runs. This  
542 method provides a straightforward approach to solving MO optimisation problems because the ILP  
543 formulations are relatively simple to provide as input when compared to the requirements of heuristics  
544 such as the NSGA-II – which include sophisticated code and multiple parameters that require iterative  
545 tuning and an intimate knowledge of their effects. A strong characteristic of the weighted-sum approach  
546 is that the end-points of the Pareto front, which optimise with respect to only a single objective while  
547 ignoring the others, may be determined exactly. These end-points provide an indication of where the true  
548 Pareto front lies – and avoids a known weakness of MO heuristics which struggle to reach end-point  
549 regions (Kim et al., 2008).

550 The weighted-sum approach does, nevertheless, hold disadvantages. Evenly distributed weights may  
551 result in an unevenly distributed Pareto front approximation, and while truly optimal solutions can be  
552 found for the specific weight combinations, there is no guarantee that the returned solutions are on the  
553 true Pareto front (Khan and Rehman, 2013; Marler and Arora, 2010). Furthermore, assigning suitable  
554 weights to the objectives is a laborious and sensitive iterative process, and multiple runs are required in  
555 order to approximate the Pareto front (Marler and Arora, 2004; ReVelle and Eiselt, 2005). The weighted-  
556 sum approach remains a popular choice to solve MO optimisation problems from various applications  
557 (Machairas et al., 2014; Xia et al., 2019; Yao et al., 2018). The major advantage of this approach, in a  
558 practical sense, is that the user is able to specify the desired number of solutions in the form of the number  
559 of weight combinations. Heuristics often generate an impractically large number of solutions on the  
560 Pareto front approximation, which are unrealistic to present to decision-makers (Heyns et al., 2019) and  
561 require further analysis to be reduced to a manageable number (Heyns, 2016; Mavrotas, 2009).

562 The ILP formulation of the problem is now presented and is based on the *Maximal Covering Location*  
563 *Problem* (MCLP), first proposed and formulated by (Church and ReVelle, 1974). The CWDS planning  
564 problem includes multiple covering objectives evaluated with respect to multiple CZs, for which a multi-

565 CZ formulation of the MCLP was introduced by Heyns et al. (2020). The parameters used are listed  
 566 below.

567

568  $N_t$  denotes the number of towers available for placement.

569  $N_c$  denotes the number of CZs.

570  $s$  denotes the number of candidate sites in the PZ.

571  $d_c$  denotes the index of demand points in CZ  $c$ , where  $c \in \{1, \dots, N_c\}$ .

572  $N_{d_c}$  denotes the number of demand points in CZ  $c$ .

573  $\mathbb{N}_{d_c}$  denotes the subset of sites in the PZ from which demand point  $d_c$  in CZ  $c$  is visible.

574  $x_s$  is 1 if a tower is placed at site  $s$ , and 0 otherwise.

575  $y_{d_c}$  is 1 if a demand point  $d_c$  is covered, and 0 otherwise.

576

577 The objective is to:

$$\text{maximise } V_c = \sum_{d_c} y_{d_c} \quad \forall c \in \{1, \dots, N_c\} \quad (2)$$

578

579

580 subject to the constraints:

581

$$y_{d_c} \leq \sum_{s \in \mathbb{N}_{d_c}} x_s \quad (3)$$

$$\sum_s x_s = N_t \quad (4)$$

$$x_s \in \{0,1\} \quad (5)$$

$$y_{d_c} \in \{0,1\} \quad (6)$$

582

583 The objective in (2) is to maximise cover with respect to each CZ  $c \in \{1, \dots, N_c\}$ . The constraint in (3)  
 584 allows a demand point  $d_c$  to be covered ( $y_{d_c} = 1$ ) only if one or more cameras are placed at sites in the  
 585 set  $\mathbb{N}_{d_c}$ . Constraint (4) ensures that exactly  $N_t$  towers are placed, while constraints (5) to (6) specify  
 586 binary requirements on the auxiliary variables.

587

588 To arrive at the weighted objective function, the  $N_c$  objectives in (2) can be reduced to a single function  
 589 using a weight,  $w_c$ , for each CZ. The objective is then to

590

$$\text{maximise } V = \sum_c w_c \frac{100}{N_{d_c}} \sum_{d_c} y_{d_c} \quad (7)$$

591

592 The objective in (7) is subject to the same constraints (3) to (6), enforced with respect to all CZs. The  
 593 fraction is included in the objective function to reflect the maximisation of the *percentage* of cover  
 594 achieved with respect to each CZ, so that the objective function is not biased towards larger CZs with  
 595 more demand points.

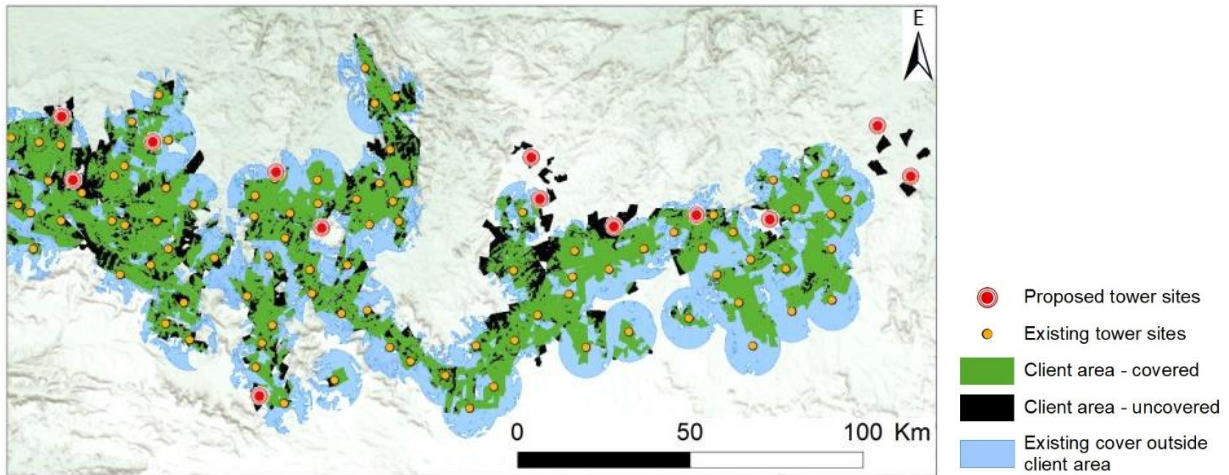
## 596 3 Data and methods

### 597 3.1 Single-site selection problem

#### 598 *3.1.1 Problem description*

599 ForestWatch requested assistance in the selection of a number of sites in the Mpumalanga Province in  
 600 December 2018. The problem did not require system optimisation – ForestWatch provided thirteen sites  
 601 proposed by planners for which individual alternatives were sought. This served as an evaluation of the

602 proposed sites, and to provide ForestWatch with alternatives if there were any that were significantly  
 603 better than the proposed ones. This provided a practical opportunity to refine the GIS component of our  
 604 framework by implementing the exploitation of landforms for the selection of superior sites, as earmarked  
 605 for later use in system optimisation problems. The locations of the proposed sites are shown by red  
 606 markers in Figure 8, along with the existing towers in the region (orange markers), the client areas already  
 607 covered by the existing towers (the green surface area) and the client areas that are not covered (the black  
 608 surface areas). The cover achieved by the existing towers outside of the client areas is indicated in blue  
 609 in the figure (using an 8 km detection range).  
 610



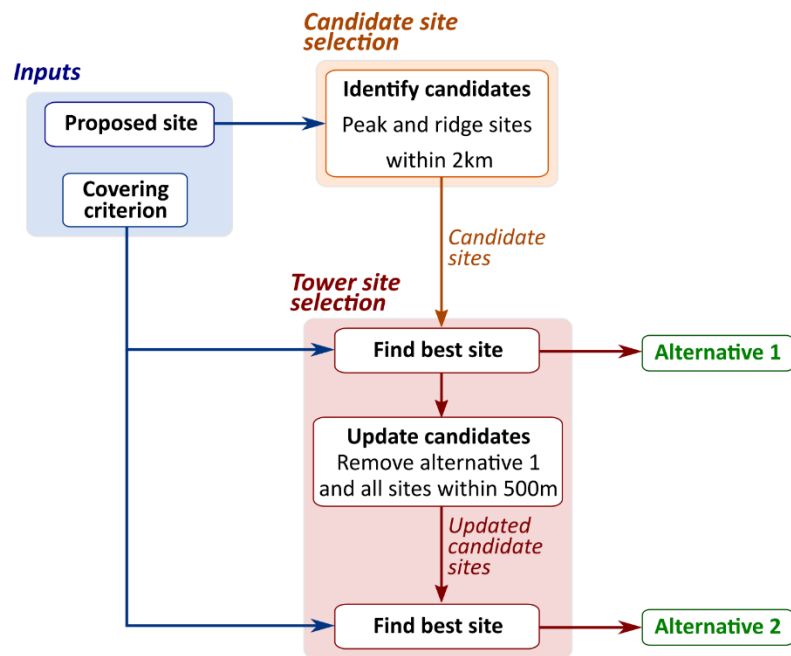
611  
 612 Figure 8 Thirteen sites (the red markers) that were proposed by ForestWatch, with the aim of providing additional cover over  
 613 client plantations and surrounding areas.

614 *3.1.2 Single-site solution framework*

615 As previously discussed, searching for superior sites within a given region is not uncommon, but  
 616 searching for alternatives for a proposed site was a challenge for which we required to develop our own  
 617 framework. Sites that were classified as peaks or ridges within a 2 km radius around each of the proposed  
 618 towers were identified as candidate alternative sites. A 2 km radius was agreed upon with decision makers  
 619 as this is typically the maximum extent around which they would consider and search for alternatives in  
 620 real-world site searches (4 km was used for one of the thirteen sites because of site-specific requirements  
 621 outlined by technicians). Road accessibility was not considered here, because obtaining the roads layers  
 622 from multiple clients in the region (with data that are typically conflicting between clients and/or  
 623 outdated) was a task that was too laborious to complete and verify within the short timeframe that was  
 624 available. Furthermore, it was decided to omit the consideration of suitable degree of slope that was  
 625 considered in previous work (Heyns et al., 2019), because peak and ridge sites inherently exhibit low  
 626 degrees of slope, as observed in Figure 5 (this was also assumed for the system-site optimisation problem  
 627 presented later).

628 Exhaustive searches were performed using the identified candidate sites around each proposed tower,  
 629 with the goal of providing multiple alternatives. To ensure this, three covering criteria were used to  
 630 evaluate each candidate site, namely a) total cover achieved (client and outside), b) total client cover  
 631 achieved (within client boundaries only), and c) total new client cover achieved (existing blind spots in  
 632 the client area). Since the aim here was single-site optimisation, no layout alternatives were required, so  
 633 only one smoke layer height of 30 m was considered for site evaluation. Recall that multiple smoke layers  
 634 serve the important purpose of returning layouts with different tower-site location combinations, but this  
 635 is not required here and the three covering objectives (at 30-m heights) are considered sufficient to return  
 636 alternatives. Our framework is described next, and is illustrated in Figure 9 – repeated with respect to  
 637 each covering criterion. As seen in the figure, once all candidate alternatives around each proposed site  
 638 is identified and evaluated with respect to a criterion, two alternatives are identified. This is achieved by  
 639 identifying the best-performing alternative with respect to a criterion – alternative 1 – after which this site

640 and all others within 500 m are removed from the candidates, and the second-best alternative is identified  
 641 from the remaining alternatives – alternative 2. The requirement of at least 500 m between the first and  
 642 second-best alternatives is enforced to ensure that neighbouring sites are not proposed as first and second-  
 643 best alternatives (neighbouring sites typically exhibit similar visibility results). This also ensures  
 644 diversity in the locations of alternative site locations – and therefore more alternatives for decision-  
 645 makers.



646  
 647 Figure 9 The single-site search framework used to determine alternative sites around a proposed site, determined with respect to  
 648 a covering criterion – the framework is repeated for each criterion. In our application, three criteria were considered, and two  
 649 alternatives were sought with respect to each criterion.

## 650 3.2 System-site selection problem

### 651 3.2.1 Problem description

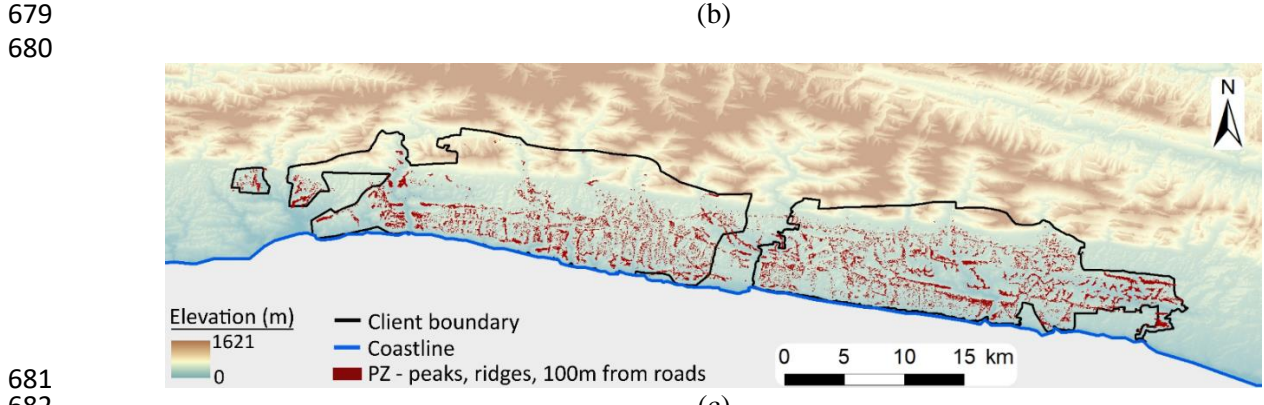
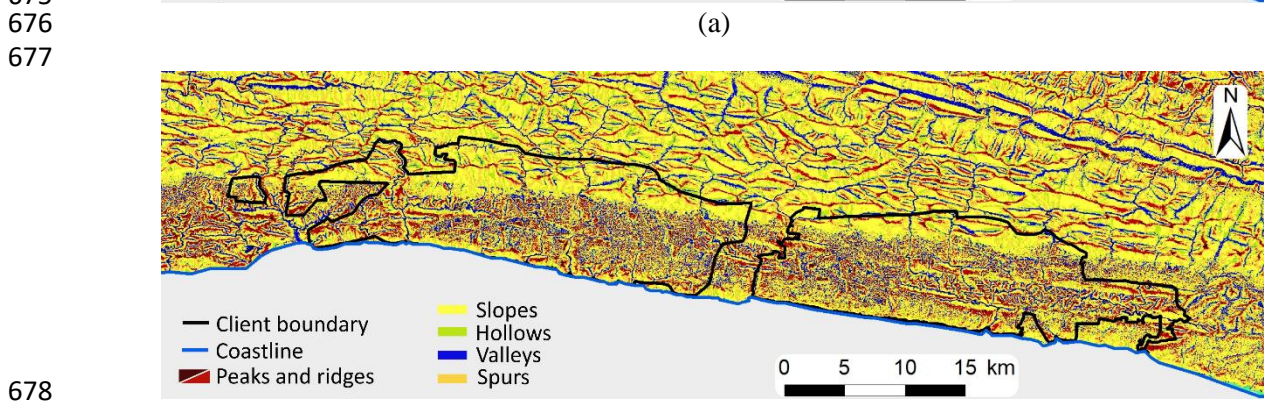
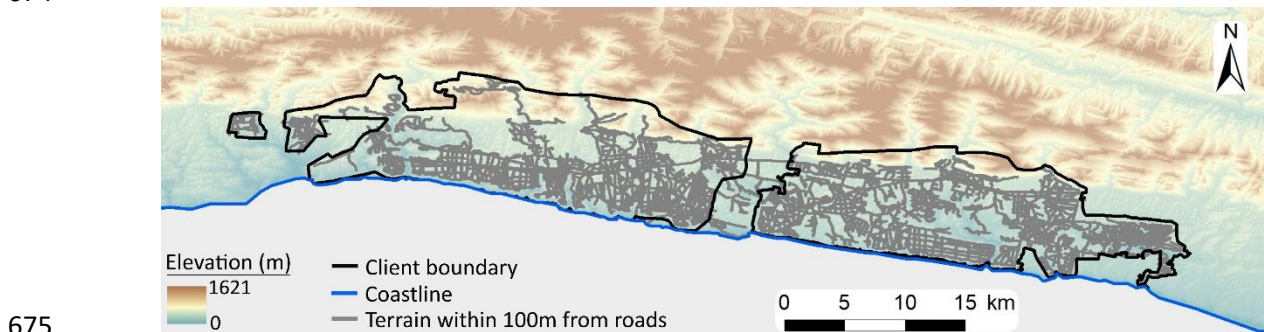
652 In May 2019, ForestWatch requested optimal CWDS site locations to provide coverage to a forestry client  
 653 in South Africa’s Southern Cape (a total of 435 sq. km of client property), 60 km away from where the  
 654 devastating 2017 Knysna fires occurred (Forsythe et al., 2019). Alternatives were sought to compare to  
 655 a four-site layout that had been determined by ForestWatch technicians following weeks of speculation  
 656 and physical site exploration. They had to propose a layout to their client within less than a week and  
 657 requested an evaluation of their proposed layout and an additional investigation to identify possible  
 658 superior alternatives. This meant that there was only enough time to implement the first stage of the  
 659 optimisation framework (MRA-NSGA-II) to obtain alternatives, without any additional optimisation runs  
 660 as has been performed in previous work (Heyns et al., 2019, 2020). As will be shown later, this did not  
 661 have any significant impact on the solution quality of the layouts.

### 662 3.2.2 Preliminary analyses

663  
 664 The client boundaries are displayed in **Error! Reference source not found.**(a), in addition to the terrain  
 665 surface that lies within 100 m from roads, indicated in grey. Roads data were obtained for those roads  
 666 from which it was permissible to place towers – although some roads lie outside and between the two  
 667 large client areas, permission was granted to consider this area for site placement due to agreements with  
 668 ForestWatch and local authorities. Geomorphons were determined for the terrain surface, illustrated in  
 669 Figure 10(b) (note that the legend only shows the main visible landform types and the others are not  
 670 shown because of their scarcity). All sites that were identified to be within 100 m from roads and  
 671 classified as peaks or ridges by the geomorphon approach were included in the final PZ, illustrated in



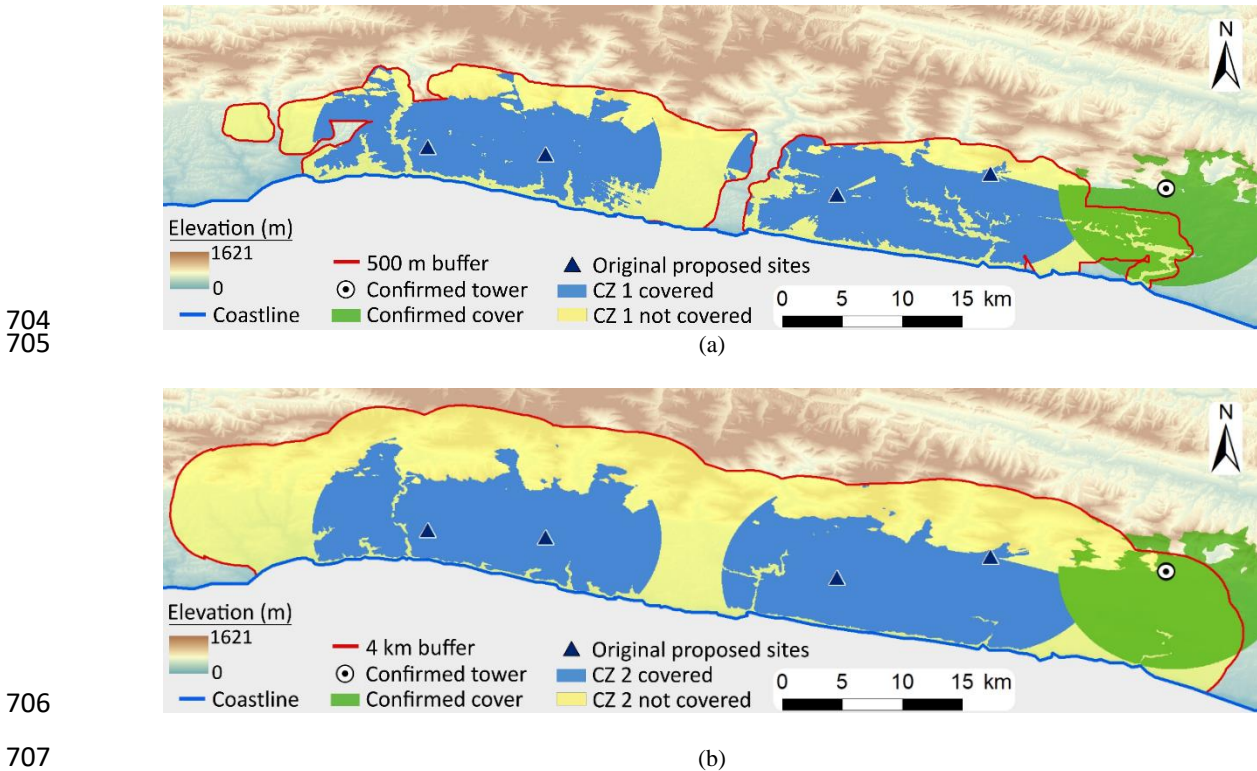
672 Figure 10(c). This PZ contained 46 483 sites (30-m resolution), which was reduced down to 5 172 at the  
 673 lower 90-m resolution for the MRA.  
 674



683 Figure 10 Process for identifying the PZ for the Southern Cape site-selection problem. (a) Client boundaries and terrain within  
 684 100 m of roads (in grey), considered for accessibility purposes. (b) Geomorphon classification of the Southern Cape terrain (only  
 685 the most notably visible landforms are provided in the legend). (c) The final selection of candidate sites (final PZ).

686 Two CZs were considered, namely (a) 30 m above plantations with a 500 m buffer (immediate detection),  
 687 and (b) 100 m above plantations with a 4 km buffer (secondary detection). Additionally, it was requested  
 688 that the analysis complemented the cover achieved from a pre-selected tower, located slightly outside and  
 689 to the east of the client’s boundaries. This tower site was previously confirmed, meaning that certain  
 690 portions of the smoke layers and buffers would already be covered by a camera there, so these covered  
 691 areas were excluded from the remaining cover demand. In Figure 11 the CZ boundaries are shown, along  
 692 with the location and cover achieved by the pre-determined camera, as well the coverage achieved by the  
 693 ForestWatch-proposed site locations. The coverages were determined with a camera range of 8 km and  
 694 proposed tower heights of 36 m, 24 m, 24 m, and 12 m, when moving from left to right in the images.  
 695 The confirmed tower’s coverage was determined at its proposed tower height of 24 m. It was determined  
 696 that the four-tower layout proposed by ForestWatch experts would achieve cover of 58.9% and 45.8%  
 697 with respect to the uncovered areas of CZ1 and CZ2, respectively. Noteworthy are the gaps in coverage  
 698 that exist at 30 m in Figure 11(a) that are filled when the coverage of the towers are evaluated at 100 m  
 699 in Figure 11(b). Clear examples exist to the southeastern corner of the cover achieved by the second-

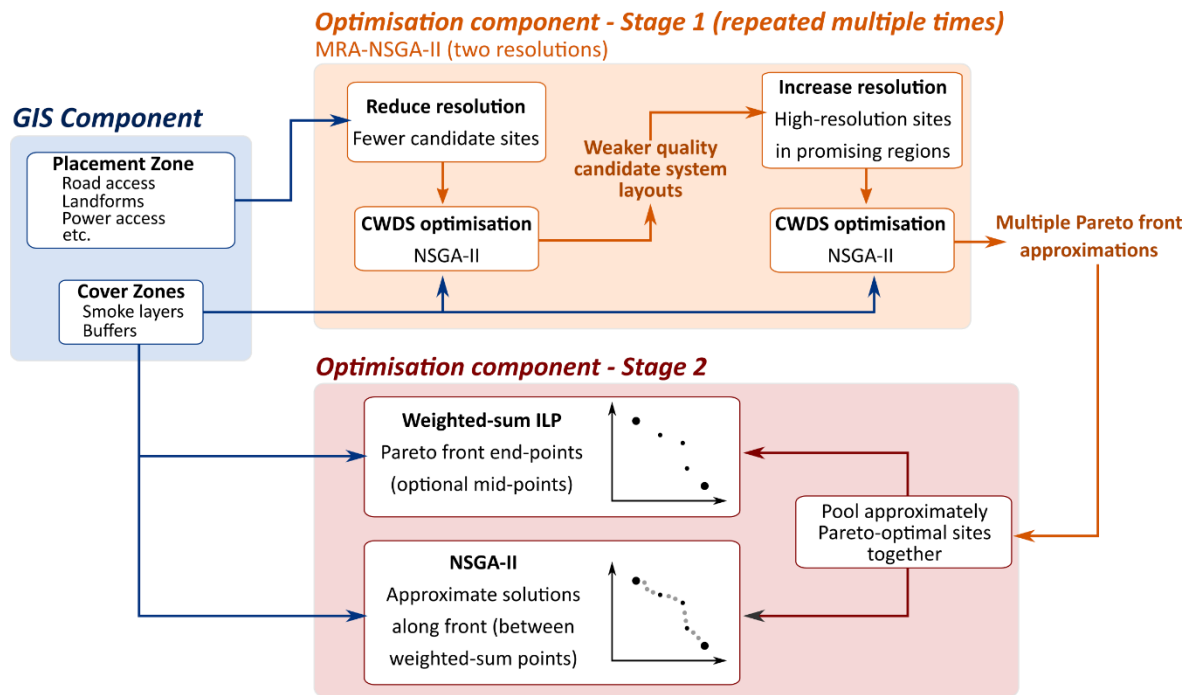
700 from-left tower, while also clearly visible to the south of the fourth-from-left tower. This shows that the  
 701 CZs are not merely the client boundaries with extended buffer zones, but that the concept of determining  
 702 smoke coverage at different heights above the terrain does indeed influence the coverage results.  
 703



708 Figure 11 Site locations and cover achieved for the CWDS layout originally proposed by ForestWatch. Cover achieved with  
 709 respect to (a) CZ1 and (b) CZ2.

### 710 3.3 System-site solution framework

711 As discussed before, both the use of heuristics and a weighted-sum approach have advantages and  
 712 disadvantages. The use of heuristics is expected to continue forming the basis of the first optimisation  
 713 stage, especially considering the general size of solution spaces considered in our problems. For the  
 714 second stage, in which a weighted-sum approach is possible, we propose a combined approach – differing  
 715 from our previous research in which the second stage involved either heuristics (Heyns et al., 2019) or  
 716 ILP (Heyns et al., 2020), but not both. The benefits of a combined approach are numerous, and are  
 717 demonstrated in the results presented later. Briefly, the weighted-sum approach may be used to  
 718 determine, at the very least, the end-points of the Pareto front to provide an indication of its extent. We  
 719 then employ both heuristics and the weighted-sum approach to determine solutions along the front,  
 720 between the end-points. Instead of choosing one approach over the other, the weighted-sum approach  
 721 can be used to approximate the general shape of the front, while the heuristic approach can be used to  
 722 find numerous additional solutions between these points. Selected heuristic solutions may be proposed  
 723 to decision-makers if their solution quality is considered acceptable when compared to the Pareto front’s  
 724 weighted-sum solutions, while weighted-sum solutions may, of course, also be proposed. An overview  
 725 of the site-selection framework, divided into the GIS component and its two stages of the optimisation  
 726 component, is provided in Figure 12.  
 727



728

729  
730

Figure 12 The CWDS tower site-selection optimisation framework, comprising a GIS component and two stages of optimisation components.

731 **4 Results**

732 **4.1 Single-site alternative searches**

733 Since three criteria were considered and two alternatives were sought for each, a total of six alternative  
734 sites were to be expected for each proposed site. However, many alternative sites were discovered with  
735 respect to more than one criterion – e.g. an alternative site offering the best total cover also being found  
736 to offer the best client cover. Generally, at least four alternatives were identified for each site. In the  
737 worst-case scenario, two sites were found as alternatives – one site achieved the best coverage with  
738 respect to each criterion, while the other achieved the second-best with respect to each.

739

740 The coverage results of the proposed sites and their alternatives are displayed in Table 1 and an example  
741 of the presentation of the results that were provided to decision makers is displayed in Figure 13. The  
742 alternative site locations were exported to be viewable in Google Earth, and each alternative’s coverage  
743 values and viewsheds could be toggled on and off by clicking on its icon. Also viewable in the figure is  
744 the covered client area (shaded green) and the uncovered client area (shaded red), upon which the towers’  
745 coverage maps could be viewed and appraised.

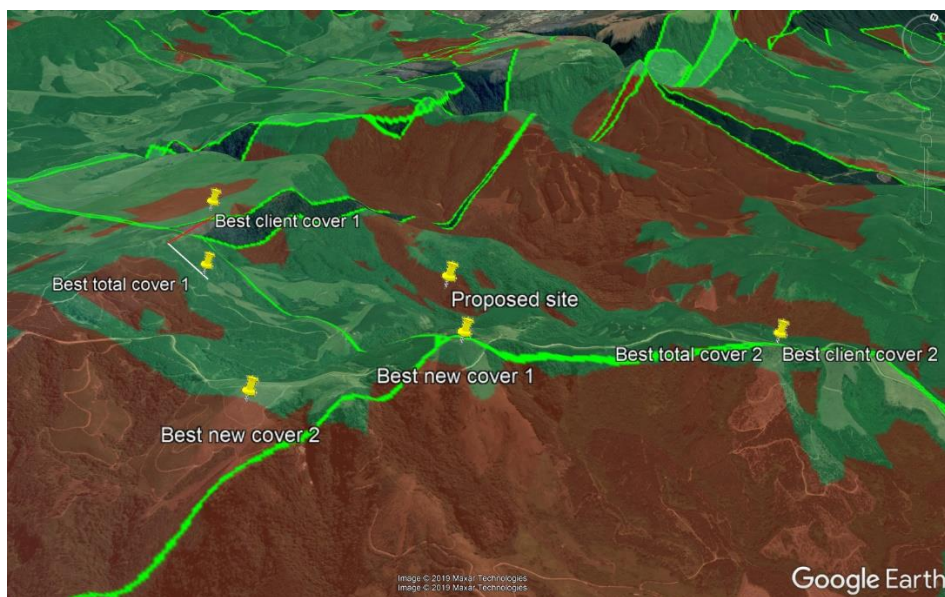
746

747 The first six towers that are listed Table 1 (along the rows) are those for which the decision-makers chose  
748 one of our alternatives above their proposed sites. These selected alternatives are displayed in bold  
749 (sometimes identified as a superior alternative with respect to two criteria), and sites that were identified  
750 with respect to multiple criteria are indicated by asterisks (corresponding to the number of asterisks).  
751 Decision-makers explained that the six alternative sites were selected because of superior coverage and,  
752 in some instances, superior accessibility compared to the initially proposed sites. Regarding the  
753 remaining sites that the decision-makers chose to keep instead of choosing an alternative, in all instances  
754 these sites achieved inferior cover, but the decision-makers preferred them to alternatives due to either  
755 existing infrastructure or accessibility. The total hectares covered for each tower-criterion combination  
756 are displayed at the bottom of Table 1, and the total percentage improvement that was achieved by the  
757 alternatives compared to that achieved by the proposed towers with respect to each criterion are also  
758 displayed. The most significant value here is the almost 20% improvement in client cover that was  
759 determined to be possible with the alternatives.

760 Table 1 Summary of the coverage results of the single-site alternative search for 13 towers in the Mpumalanga province.  
 761 Alternatives that were selected in favour of the proposed sites are displayed in bold, while sites that were identified with respect  
 762 to multiple criteria are indicated by the number of asterisks.

Tower name and number	Proposed tower cover (hectares)			Alternatives – total cover (hectares)		Alternatives – client cover (hectares)		Alternatives – new cover (hectares)	
	Total	Client	New	Best	Second	Best	Second	Best	Second
Dundonald 1	9705	4401	2027	<b>12754*</b>	11853**	4719	4715**	<b>2739*</b>	2582
Zwalusnest 2	14089	2106	2095	14169*	<b>13784</b>	2111*	2060	2100*	2048
Blairmore 3	14365	10838	5983	16052	15825	13646	13159	<b>6204</b>	6144
Mkhondo 4	15699	1641	1546	17445	<b>17288*</b>	2620	2425	<b>2054*</b>	1969
Ridges 5	15502	5019	198	<b>15502</b>	14473	7197	6761	267	232
Derby 6	12501	7200	1801	<b>16073*</b>	15973**	<b>9850*</b>	9771**	1993	1980
Ntabanyama 7	10761	6248	847	12393*	11011**	7193*	6360**	891*	868**
Klipkopjie 8	14892	8826	608	16483*	16129	10194*	9738	721	678
Potgieterskeurs 9	15841	1170	1164	15949	15561	1211*	1195	1205*	1191
World's View 10	11028	10412	5148	12587*	12336**	11945*	11681**	5421	5117
Mac Mac 11	12575	6381	2208	13028*	11496**	6472	6311	2309*	1823**
Van Staden 12	14412	6169	941	14464	14112	7184	6747*	1206	1151*
Snymansbult 13	12742	6196	958	14091*	13802	7258	7121	1150	1133*
<b>Total (ha)</b>	174112	76607	25524	190990	183643	91600	88044	28260	26916
<b>Improvement (%)</b>				9.7	5.5	19.6	14.9	10.7	5.5

763



764

765 Figure 13 An illustration of solutions provided to decision makers in the single-site alternative search problems. Multiple  
 766 alternatives were exported to view Google Earth and their coverage values and coverage maps could be toggled on and off by  
 767 clicking on each alternative site (not illustrated in the figure). Coverage maps could be viewed and compared relative to the  
 768 covered client areas (green shaded within green boundaries) and the uncovered client areas (the red shaded areas).

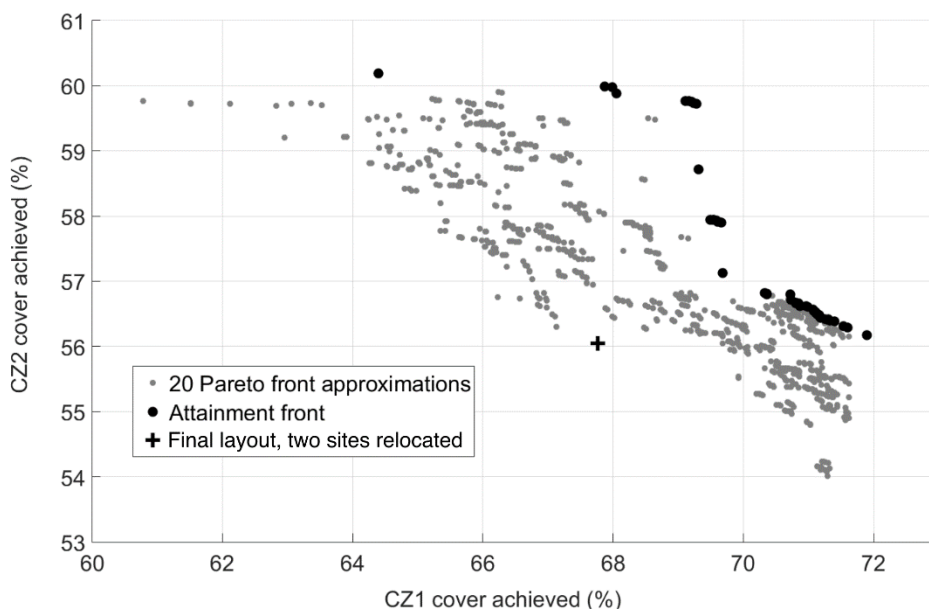
769 The files that were provided to ForestWatch and viewable as in *Figure 13* are available online (Heyns,  
 770 2020) and can be viewed with Google Earth Pro software. The user can toggle client areas, uncovered  
 771 areas, and the thirteen sites and their alternatives' locations and viewsheds. Note that the Mkhondo  
 772 alternative site search was expanded to 4 km instead of the 2 km used for all the other sites, due to specific  
 773 technician request.

#### 774 4.2 Southern Cape four-tower system

775 Twenty Pareto front approximations were performed with the MRA-NSGA-II, and their results and the  
 776 final attainment front (the set of best solutions from all runs) are provided in Figure 14. A number of

777 layouts from the attainment front were provided to decision makers and presented in a manner similar to  
 778 that of the single-site selection process displayed in Figure 13 – layouts were exported to be viewable in  
 779 Google Earth, along with proposed cover maps above client property. The solution that achieved the best  
 780 cover with respect to CZ1 (i.e. the solution furthest to the right in Figure 13) was selected because of its  
 781 coverage, but also because the sites were located in areas that were considered accessible and practical.  
 782 The site locations and cover achieved with respect to the CZs by the two end-point solutions on the  
 783 attainment front in Figure 13 – i.e. the two solutions that perform best with respect to each objective – are  
 784 displayed in Figure 15(a) to (d) to illustrate the kind of trade-offs in site locations and cover that result  
 785 from following a MO, multi-CZ solution approach. The results were obtained within four days – including  
 786 data collection, processing, optimisation, analysis, and exports to visual presentation for decision-makers.  
 787 CZ % achieved by these solutions?  
 788

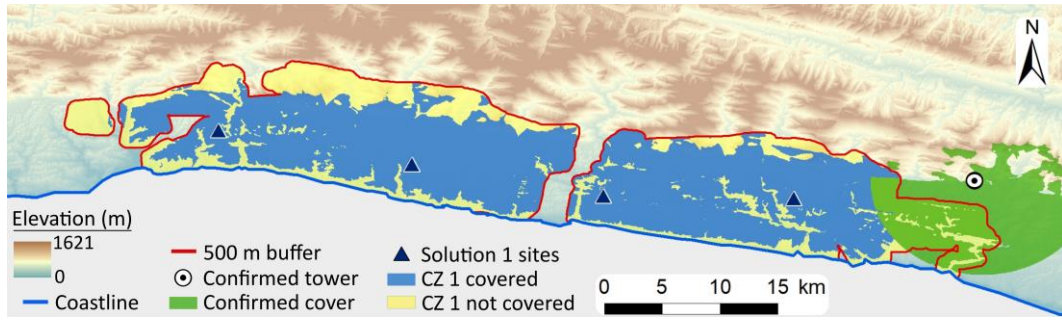
789 As may be expected in a practical environment, ForestWatch experts decided to relocate the locations of  
 790 some sites in the framework-determined solutions – the two eastern-most sites of the selected layout in  
 791 this instance. The relocations are displayed in Figure 16 and were to improve accessibility for the site in  
 792 (a) in the figure, while the site in (b) was moved to gain access to a stable power supply. These relocations  
 793 resulted in minor changes to the coverage results and the relocated layout’s objective function values are  
 794 displayed in Figure 14 (the black cross). This only reduced the cover with respect to CZ1 by 4%, while  
 795 the loss of cover with respect to CZ2 is negligible. Furthermore, compared to the layout proposed by  
 796 decision makers, this final, relocated layout achieves an improvement of 9% in cover with respect to CZ1  
 797 and 10% with respect to CZ2, (not forgetting that the initial layout is evaluated at taller proposed tower  
 798 heights, while the final layout is evaluated with 12-m towers).  
 799



800  
 801 Figure 14 Pareto-front approximations of twenty heuristic runs (the grey dots) and the resulting attainment front (the black dots).

802  
 803  
 804  
 805  
 806

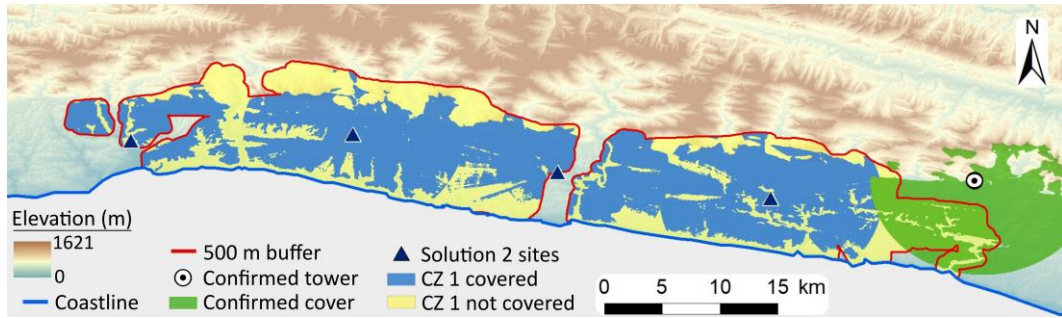
807



808

(a)

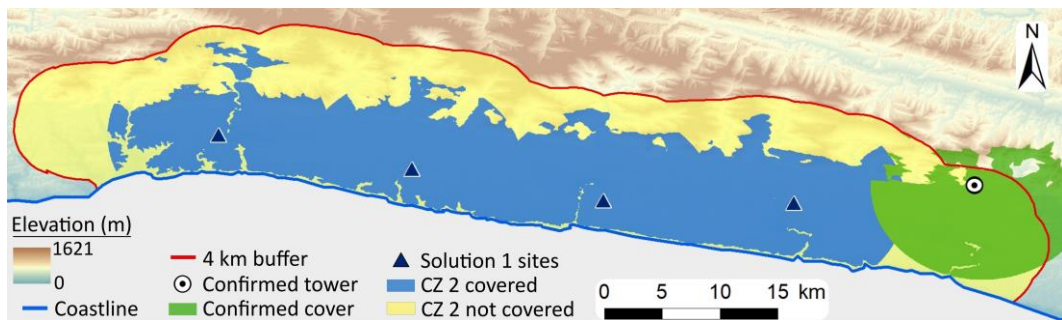
809



810

(b)

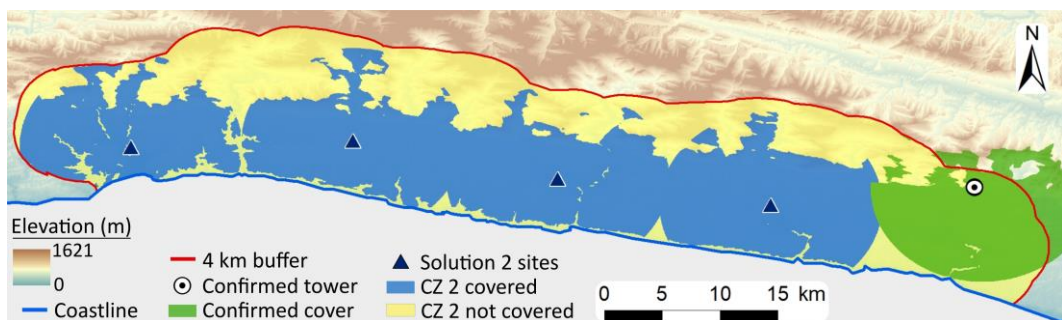
811



812

(c)

813



814

(d)

815

816

Figure 15 Site locations and cover achieved for the solutions from Figure 14 that achieve the best cover with respect to CZ1 (solution 1) and CZ2 (solution 2). Cover achieved with respect to CZ1 in (a) and (b), and CZ2 in (c) and (d).



817  
818

(a)

(b)

819 Figure 16 Relocations imposed by decision makers on the two eastern-most sites of the proposed layout in Figure 15(a) and (c)  
820 (solution 1). The relocation in (a) was for improved accessibility, while that in (b) was to gain access to a stable power supply.

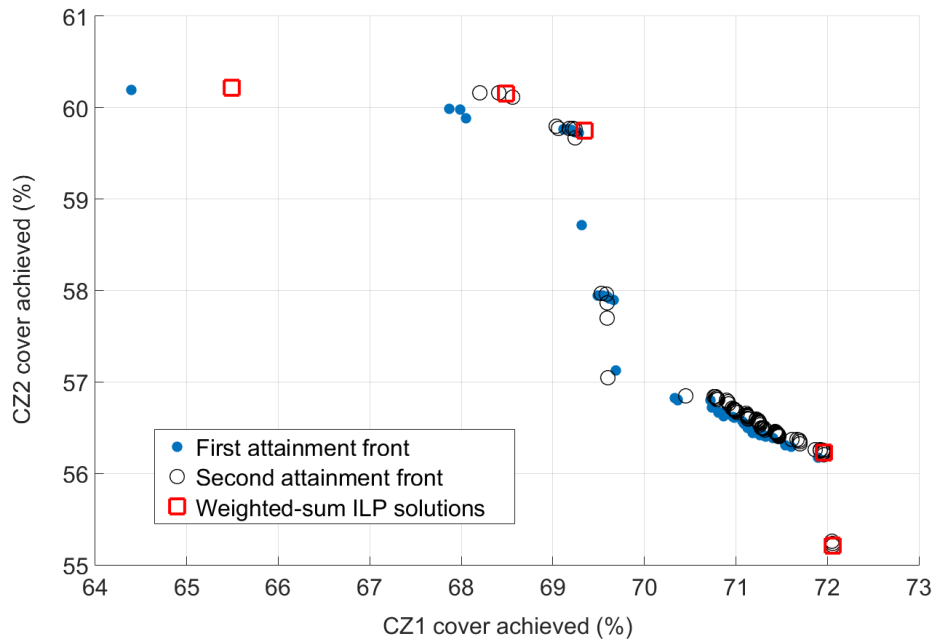
821 Files for some of results presented here are available online (Heyns, 2020), and viewable in Google Earth  
822 Pro. These include the client areas, areas covered by the pre-specified tower, the CZs, and the site  
823 locations and viewsheds of the two solutions viewable in Figure 15. The two altered site locations as in  
824 Figure 16 are also provided.

### 825 4.3 Post-optimisation analysis

826 The Southern Cape CWDS site selection problem was performed within a limited timeframe and only the  
827 first stage of the optimisation component could be completed. The second stage of the optimisation  
828 component was performed afterwards to investigate what results could have been obtained if the full  
829 framework had been implemented, and to evaluate the quality of the solutions that had been proposed.

830  
831 All the sites contained in the solutions in the twenty Pareto front approximations in Figure 14 were pooled  
832 together, resulting in a small PZ of 363 candidate sites. Ten additional runs of the NSGA-II were  
833 performed with this PZ as input and the attainment front achieved by these runs is provided in Figure 17  
834 (the empty black markers). Furthermore, the same PZ was used as input to a weighted-sum ILP approach,  
835 with the following weights used for the two objectives presented in the format (CZ1, CZ2): (1.00,0.00),  
836 (0.75,0.25), (0.5,0.5), (0.25,0.75), (0.00, 1.00). The first and last weight sets effectively examine the  
837 optimal solution for a single CZ. The resulting solutions for this approach are shown in Figure 17 by the  
838 red markers. Of note is that there appears to be no real improvement in the quality of the solutions  
839 obtained by the first optimisation stage (the blue markers) and those from the second stage. The  
840 explanation for this is a smaller number of towers to place and a significantly smaller PZ than investigated  
841 in the Nelspruit problems (Heyns et al., 2019, 2020) in which the second optimisation stage demonstrated  
842 conspicuous improvement – here, 4 towers to place compared to 20, and 46 483 candidate sites compared  
843 to 741 813. The smaller computational complexity therefore results that the first, MRA-NSGA-II  
844 optimisation stage is able to obtain high quality site combinations.

845



846

847 Figure 17 Pareto-front approximation attainment fronts obtained by additional heuristic and weighted-sum ILP runs from the  
848 second stage of the optimisation component.

849 The second-stage results demonstrate some of the disadvantages of both approaches. As previously stated  
850 and as may be seen here, evenly distributed ILP weights nevertheless result in an unevenly distributed  
851 weighted-sum Pareto front approximation. This is because of the changes in shape from concave (outer  
852 areas) to convex (the large gap area between two solutions), as has been described in the literature – see  
853 e.g. (Li and Yao, 2017). Nevertheless, the weighted-sum solutions provide us with an indication of where  
854 the true optimal front lies (at least for the 363 sites in the smaller PZ). This allows the quality of the  
855 heuristic-determined solutions to be better appraised. Concerning the solutions from the second-stage  
856 heuristic-determined front, it is clear that they exhibit similar solution quality compared to those offered  
857 by the weighted-sum front. The heuristic front includes a solution that matches one of the end-points of  
858 the weighted-sum front, but fails to reach the other – a known weakness of the heuristic approach (Kim  
859 et al., 2008). Furthermore, many solutions on the final heuristic front is observed (88 solutions). Such a  
860 large number of solutions is impractical for decision making purposes and many are clustered closely  
861 together and do not offer significant trade-offs in objective function values, nor tower site locations.  
862 Nevertheless, the front does discover numerous solutions otherwise overlooked in the gap of the  
863 weighted-sum front. Such solutions could offer coverage and tower site locations that may be of interest  
864 to decision makers in a practical environment, which can be overlooked if only a weighted-sum approach  
865 is followed.

866

867 The above observations illustrate how the approach of combining heuristic and weighted-sum analyses is  
868 capable of revealing important Pareto front characteristics and solution analysis to support CWDS  
869 decision-making and should certainly prevail in future problems.

## 870 5 Discussion

871 The results obtained for the single-site alternative searches and the system-optimisation problem were all  
872 well-received by decision-makers. The alternative search framework provided decision-makers with  
873 practical solutions which they could consider, and they appreciated the manner in which they could  
874 compare sites in Google Earth and visually display different site viewsheds. Unfortunately, ForestWatch  
875 was not awarded the most recent contract for wildfire detection in the region to build on their existing  
876 towers in operation. Despite the fact that the towers identified here may not be constructed, the purpose  
877 of our framework is to determine sites that can help ForestWatch decision-makers in selecting final sites,  
878 in real-world problems. This was achieved because the sites that were determined with the aid of our  
879 framework were those that were confirmed to be built if the contract was awarded.



880 The system-site selection framework was applied to solve a bi-objective CWDS placement problem in  
881 the Southern Cape – with the maximisation of coverage of each CZ as an objective – using MO  
882 optimisation solution approaches. Feedback from decision makers involved in this problem was that the  
883 solutions allowed them to spend their time on refining site locations, as opposed to performing rigorous  
884 practical site searches with no starting point at all. Furthermore, the coverage maps and the coverage  
885 values in hectares that are exported to be easily viewed in Google Earth make it possible to easily analyse  
886 and compare – and the nature of the proposed data and their presentation give the clients assurance that  
887 best efforts have been made in finding optimal sites. At the time of writing, completion of the contract  
888 in the area is still pending and has been delayed by the client due to economic factors, further exacerbated  
889 by Covid-19. Nevertheless, the goal of providing practical tower sites by the framework to aid decision-  
890 makers has been achieved. The sites proposed by our framework as presented in this paper – and agreed  
891 upon between ForestWatch and the client – will be used as soon as (and if) the contract finally proceeds.  
892

893 In future problems it is expected that additional (or alternative) objectives may be considered. One  
894 example is that of proximity to power supplies. In the Southern Cape exercise, proximity from power  
895 was not considered as a constraint in determining PZ sites because of typical problems that ForestWatch  
896 have experienced with power outages and their preference for installing towers with solar power supplies.  
897 As was observed during solution analysis and selection, however, experts decided to move one tower  
898 from their preferred layout to another because of access to power. It is therefore expected that power  
899 proximity should not be used as a limiting constraint on PZ identification – instead, the minimisation of  
900 distance to power supplies should be considered as an additional *objective*. Decision-makers may then  
901 consider distance to power along with covering objectives in their analysis of Pareto-front solutions. An  
902 alternative approach would be to continue determining solutions without power supply considerations  
903 and, instead, perform local “fine-tuning” of solutions. This can be performed by automated search  
904 algorithms which determining the closest power supply point to each tower in a solution and if it is within  
905 a suitable distance, the site in the solution may be exchanged for the nearest suitable site to the power  
906 supply, and the effect on the coverage results determined. If the changes are within an acceptable  
907 threshold, then the new site may be kept.

908 Additional CZs which may be considered in future problems include certain priority areas within the  
909 larger client area, e.g. areas around key infrastructure points such as power plants and chemical storage  
910 facilities, or areas that are historically fire-prone. In such instances, a priority CZ is simply added as an  
911 additional covering objective and the problem solved as usual by the MO optimisation framework.  
912 Furthermore, alternative or additional objectives that may be considered include those that were  
913 investigated in the single-site searches, namely 1) total coverage, 2) client coverage, and 3) new client  
914 coverage – as opposed to smoke layers at different heights.

915 A set of solutions that is diverse in respect of objective function values and tower site locations are desired  
916 for decision makers. It is, however, possible that attainment fronts consisting of an undesirably large  
917 number of solutions may be returned, as was observed during the Southern Cape post-optimisation  
918 analysis. Many of the solutions appear in “clusters” and offer negligible trade-offs in terms objective  
919 function values and facility site locations. In these instances, reduction techniques may be considered to  
920 filter the Pareto front to an acceptable number of solutions. Such techniques include those that are  
921 performed in objective function space, such as the epsilon-grid method (Mavrotas, 2009), or those  
922 performed in physical solution space, such as site-proximity de-clustering (Heyns, 2016) – a combination  
923 of such techniques also merits investigation.

## 924 6 Conclusion

925 The development of two comprehensive CWDS tower-site selection optimisation frameworks for single-  
926 site alternative searches and system-site optimisation for implementation in vast, unknown territories has  
927 been described and practically applied in South Africa. The main aims of the framework are to determine  
928 multiple candidate CWDS layouts within short timeframes with minimal user input. First, the single-site

929 selection problem provided a foundation for the development of the GIS component, and also contributed  
930 to the process of visualising solutions to decision makers. Numerous alternative sites were found for  
931 thirteen sites proposed by ForestWatch, and six of their initially proposed sites were discarded for one of  
932 our proposals. Second, in the Southern Cape region, the framework obtained numerous superior solutions  
933 as alternatives to a four-tower layout proposed by ForestWatch (which required weeks of speculation and  
934 planning to determine). Our alternatives were determined by the framework within four days. Multiple  
935 proposed system layouts and coverage maps were presented to decision-makers, who selected one of our  
936 proposed solutions due to its superior cover and practical tower site locations. The layouts obtained by  
937 the optimisation framework were found to significantly outperform the initial layout with respect to both  
938 covering objectives – despite the optimisation solutions being limited to 12-m tower heights while the  
939 proposed system had an average tower height of 24 m. The fact that the installation cost of a 12-m tower  
940 is less than half that of a 24-m tower is an indication of the potential cost savings that may be achieved by  
941 the optimisation approach.

942 Going forward, the frameworks are planned for implementation in future ForestWatch site-selection  
943 problems, with numerous opportunities for improvement as described in the discussion.

## 944 7 Acknowledgements

945 The authors would like to express their sincere thanks to Mr Dennis Lawrie, Mr Dave Kuhl, Mr Adrian  
946 Daniel and Mr Gareth Perks of ForestWatch for their valuable discussions, suggestions and timely data  
947 provision during the development of our framework.

## 948 8 References

- 949 Alp, O., Erkut, E., Drezner, Z., 2003. An Efficient Genetic Algorithm for the p-Median Problem. *Annals*  
950 *of Operations Research* 122, 21–42. <https://doi.org/10.1023/A:1026130003508>
- 951 Bao, S., Xiao, N., Lai, Z., Zhang, H., Kim, C., 2015. Optimizing watchtower locations for forest fire  
952 monitoring using location models. *Fire Safety Journal* 71, 100–109.  
953 <https://doi.org/10.1016/j.firesaf.2014.11.016>
- 954 Church, R., ReVelle, C., 1974. The maximal covering location problem. *Papers of the Regional Science*  
955 *Association* 32, 101–118.
- 956 Cohon, J.L., 1978. *Multiobjective Programming and Planning*. Academic Press, New York (NY).
- 957 Deb, K., Pratap, A., Agarwal, S., Meyarivan, T., 2002. A fast and elitist multiobjective genetic algorithm:  
958 NSGA-II. *IEEE Transactions on Evolutionary Computation* 6, 182–197.  
959 <https://doi.org/10.1109/4235.996017>
- 960 Di Stefano, M., Mayer, L., 2018. An Automatic Procedure for the Quantitative Characterization of  
961 Submarine Bedforms. *Geosciences* 8, 28. <https://doi.org/10.3390/geosciences8010028>
- 962 Djurdjevac Conrad, N., Helfmann, L., Zonker, J., Winkelmann, S., Schütte, C., 2018. Human mobility and  
963 innovation spreading in ancient times: a stochastic agent-based simulation approach. *EPJ Data*  
964 *Science* 7. <https://doi.org/10.1140/epjds/s13688-018-0153-9>
- 965 Eugenio, F.C., Rosa dos Santos, A., Fiedler, N.C., Ribeiro, G.A., da Silva, A.G., Juvanhol, R.S., Schettino,  
966 V.R., Marcatti, G.E., Domingues, G.F., Alves dos Santos, G.M.A.D., Pezzopane, J.E.M., Pedra,  
967 B.D., Banhos, A., Martins, L.D., 2016. GIS applied to location of fires detection towers in  
968 domain area of tropical forest. *Science of The Total Environment* 562, 542–549.  
969 <https://doi.org/10.1016/j.scitotenv.2016.03.231>
- 970 Fonseca, C.M., Fleming, P.J., 1993. Genetic algorithms for multiobjective optimization: Formulation,  
971 discussion and generalization, in: *Proceedings of the Fifth International Conference on Genetic*  
972 *Algorithms*. pp. 416–423.
- 973 Forsythe, G., Le Maitre, D., van den Dool, R., Walls, R., Pharoah, R., Fortune, G., 2019. The Knysna Fires  
974 of 2017: Learning from this disaster [WWW Document]. URL  
975 [https://www.polity.org.za/article/the-knysna-fires-of-2017-learning-from-this-disaster-2019-](https://www.polity.org.za/article/the-knysna-fires-of-2017-learning-from-this-disaster-2019-06-07)  
976 [06-07](https://www.polity.org.za/article/the-knysna-fires-of-2017-learning-from-this-disaster-2019-06-07) (accessed 12.18.19).
- 977 Franklin, W.R., 2002. Siting observers on terrain, in: Richardson, D.E., van Oosterom, P. (Eds.),  
978 *Advances in Spatial Data Handling*. Springer Berlin Heidelberg, Berlin, Heidelberg, pp. 109–120.  
979 [https://doi.org/10.1007/978-3-642-56094-1\\_9](https://doi.org/10.1007/978-3-642-56094-1_9)
- 980 Franklin, W.R., Clark, R., 1994. Higher isn't necessarily better: Visibility algorithms and experiments, in:  
981 *Advances in GIS Research: Sixth International Symposium on Spatial Data Handling*. Taylor &  
982 Francis, pp. 751–770.
- 983 Harmon, B.A., Petrasova, A., Petras, V., Mitasova, H., Meentemeyer, R., 2018. Tangible topographic  
984 modeling for landscape architects. *International Journal of Architectural Computing* 16, 4–21.  
985 <https://doi.org/10.1177/1478077117749959>
- 986 Heyns, A.M., 2020. Google Earth client and viewshed files for ITOR paper [WWW Document]. URL  
987 <http://www.andriesheyns.com/ITOR.zip> (accessed 11.23.20).
- 988 Heyns, A.M., 2016. A multi-objective approach towards geospatial facility location (Author PhD  
989 Thesis). Stellenbosch University, Stellenbosch.
- 990 Heyns, A.M., du Plessis, W., Curtin, K.M., Kosch, M., Hough, G., 2020. Analysis and exploitation of  
991 landforms for improved optimisation of camera-based wildfire detection systems. *Fire*  
992 *Technology Under Review*.
- 993 Heyns, A.M., du Plessis, W., Kosch, M., Hough, G., 2019. Optimisation of tower site locations for  
994 camera-based wildfire detection systems. *International Journal of Wildland Fire* 28, 651–665.
- 995 Heyns, A.M., Van Vuuren, J.H., 2018. Multi-type, multi-zone facility location. *Geographical Analysis* 32,  
996 3–31. <https://doi.org/10.1111/gean.12131>

997 Heyns, A.M., van Vuuren, J.H., 2016. A multi-resolution approach towards point-based multi-objective  
998 geospatial facility location. *Computers, Environment and Urban Systems* 57, 80–92.  
999 <https://doi.org/10.1016/j.compenvurbsys.2016.01.007>

1000 Heyns, A.M., Van Vuuren, J.H., 2015. An evaluation of the effectiveness of observation camera  
1001 placement within the MeerKAT radio telescope project. *The South African Journal of Industrial*  
1002 *Engineering* 26, 1–10. <https://doi.org/10.7166/26-2-1216>

1003 Hough, G., 2007. Vision systems for wide area surveillance: ForestWatch -- a long-range outdoor  
1004 wildfire detection system, in: TASSIE FIRE Conference Proceedings. Presented at the The Tassie  
1005 Fire Conference, Hobart, Tasmania.

1006 Jasiewicz, J., Stepinski, T.F., 2013. Geomorphons - a pattern recognition approach to classification and  
1007 mapping of landforms. *Geomorphology* 182, 147–156.  
1008 <https://doi.org/10.1016/j.geomorph.2012.11.005>

1009 Jia, H., Ordóñez, F., Dessouky, M.M., 2007. Solution approaches for facility location of medical supplies  
1010 for large-scale emergencies. *Computers & Industrial Engineering* 52, 257–276.

1011 Khan, S.A., Rehman, S., 2013. Iterative non-deterministic algorithms in on-shore wind farm design: A  
1012 brief survey. *Renewable and Sustainable Energy Reviews* 19, 370–384.  
1013 <https://doi.org/10.1016/j.rser.2012.11.040>

1014 Kim, K., Murray, A.T., Xiao, N., 2008. A multiobjective evolutionary algorithm for surveillance sensor  
1015 placement. *Environment and Planning B: Planning and Design* 35, 935–948.  
1016 <https://doi.org/10.1068/b33139>

1017 Kim, Y.H., Rana, S., Wise, S., 2004. Exploring multiple viewshed analysis using terrain features and  
1018 optimisation techniques. *Computers & Geosciences* 30, 1019–1032.  
1019 <https://doi.org/10.1016/j.cageo.2004.07.008>

1020 Kwong, W.Y., Zhang, P.Y., Romero, D., Moran, J., Morgenroth, M., Amon, C., 2014. Multi-objective  
1021 wind farm layout optimization considering energy generation and noise propagation with  
1022 NSGA-II. *Journal of Mechanical Design* 136, 1–10.

1023 Lee, J., 1994. Digital Analysis of Viewshed Inclusion and Topographic Features on Digital Elevation  
1024 Models. *Photogrammetric Engineering & Remote Sensing* 60, 451–456.

1025 Li, M., Yao, X., 2017. What Weights Work for You? Adapting Weights for Any Pareto Front Shape in  
1026 Decomposition-based Evolutionary Multi-Objective Optimisation. *arXiv:1709.02679 [cs]*.

1027 Luo, W., Liu, C.C., 2018. Innovative landslide susceptibility mapping supported by geomorphon and  
1028 geographical detector methods. *Landslides* 15, 465–474. <https://doi.org/10.1007/s10346-017-0893-9>

1030 Machairas, V., Tsangrassoulis, A., Axarli, K., 2014. Algorithms for optimization of building design: A  
1031 review. *Renewable and Sustainable Energy Reviews* 31, 101–112.  
1032 <https://doi.org/10.1016/j.rser.2013.11.036>

1033 Marler, R.T., Arora, J.S., 2010. The weighted sum method for multi-objective optimization: new  
1034 insights. *Structural and Multidisciplinary Optimization* 41, 853–862.  
1035 <https://doi.org/10.1007/s00158-009-0460-7>

1036 Marler, R.T., Arora, J.S., 2004. Survey of multi-objective optimization methods for engineering.  
1037 *Structural and Multidisciplinary Optimization* 26, 369–395. <https://doi.org/10.1007/s00158-003-0368-6>

1039 Martell, D.L., 2015. A Review of Recent Forest and Wildland Fire Management Decision Support  
1040 Systems Research. *Current Forestry Reports* 1, 128–137. <https://doi.org/10.1007/s40725-015-0011-y>

1041 Mavrotas, G., 2009. Effective implementation of the epsilon-constraint method in Multi-Objective  
1042 Mathematical Programming problems. *Applied Mathematics and Computation* 213, 455–465.

1044 Meunier, H., Talbi, E., Reininger, P., 2000. A multiobjective genetic algorithm for radio network  
1045 optimization, in: *Proceedings of the 2000 Congress on Evolutionary Computation*. IEEE, pp.  
1046 317–324.

1047 Misthos, L.M., Nakos, B., Krassanakis, V., Menegaki, M., 2018. The effect of topography and elevation  
1048 on viewsheds in mountain landscapes using geovisualization. *International Journal of*  
1049 *Cartography* 5, 44–66. <https://doi.org/10.1080/23729333.2018.1477569>

1050 Murray, A.T., Kim, K., Davis, J.W., Machiraju, R., Parent, R., 2007. Coverage optimization to support  
1051 security monitoring. *Computers, Environment and Urban Systems* 31, 133–147.  
1052 <https://doi.org/10.1016/j.compenvurbsys.2006.06.002>

1053 Nagy, G., 1994. Terrain visibility. *Computers & Graphics* 18, 763–773. [https://doi.org/10.1016/0097-8493\(94\)90002-7](https://doi.org/10.1016/0097-8493(94)90002-7)

1054

1055 O’Sullivan, D., Turner, A., 2001. Visibility graphs and landscape visibility analysis. *International Journal*  
1056 *of Geographical Information Science* 15, 221–237.  
1057 <https://doi.org/10.1080/13658810151072859>

1058 Owen, S.H., Daskin, M.S., 1998. Strategic facility location: A review. *European journal of operational*  
1059 *research* 111, 423–447.

1060 Purshouse, R.C., Fleming, P.J., 2003. Evolutionary many-objective optimisation: an exploratory  
1061 analysis, in: *The 2003 Congress on Evolutionary Computation, 2003. Presented at the The 2003*  
1062 *Congress on Evolutionary Computation, 2003. CEC ’03*, pp. 2066–2073.  
1063 <https://doi.org/10.1109/CEC.2003.1299927>

1064 Raisanen, L., Whitaker, R.M., 2005. Comparison and evaluation of multiple objective genetic  
1065 algorithms for the antenna placement problem. *Mobile Networks and Applications* 10, 79–88.

1066 Rana, S., 2003. Fast approximation of visibility dominance using topographic features as targets and  
1067 the associated uncertainty. *Photogrammetric Engineering & Remote Sensing* 69, 881–888.  
1068 <https://doi.org/10.14358/PERS.69.8.881>

1069 Rego, F.C., Catry, F.X., 2006. Modelling the effects of distance on the probability of fire detection from  
1070 lookouts. *Int. J. Wildland Fire* 15, 197–202. <https://doi.org/10.1071/WF04016>

1071 ReVelle, C.S., Eiselt, H.A., 2005. Location analysis: A synthesis and survey. *European Journal of*  
1072 *Operational Research* 165, 1–19. <https://doi.org/10.1016/j.ejor.2003.11.032>

1073 Romero, B.E., Clarke, K.C., 2018. Exploring uncertainties in terrain feature extraction across multi-  
1074 scale, multi-feature, and multi-method approaches for variable terrain. *Cartography and*  
1075 *Geographic Information Science* 45, 381–399.  
1076 <https://doi.org/10.1080/15230406.2017.1335235>

1077 Schroeder, D., 2005. Operational trial of the ForestWatch wildfire smoke detection system. *Advantage*  
1078 6, 1–7.

1079 South African Government, 2009. Forestry | South African Government [WWW Document]. URL  
1080 <https://www.gov.za/about-sa/forestry> (accessed 12.14.19).

1081 Strydom, S., Savage, M.J., 2016. A spatio-temporal analysis of fires in South Africa. *South African*  
1082 *Journal of Science* 112, 1–8. <https://doi.org/10.17159/sajs.2016/20150489>

1083 Tabik, S., Zapata, E.L., Romero, L.F., 2013. Simultaneous computation of total viewshed on large high  
1084 resolution grids. *International Journal of Geographical Information Science* 27, 804–814.  
1085 <https://doi.org/10.1080/13658816.2012.677538>

1086 Tanergüçlü, T., Maraş, H., Gencer, C., Aygüneş, H., 2012. A decision support system for locating  
1087 weapon and radar positions in stationary point air defence. *Information Systems Frontiers* 14,  
1088 423–444. <https://doi.org/10.1007/s10796-010-9269-6>

1089 Tong, D., Murray, A., Xiao, N., 2009. Heuristics in spatial analysis: A genetic algorithm for coverage  
1090 maximization. *Annals of the Association of American Geographers* 99, 698–711.

1091 Xia, J., Curtin, K.M., Huang, J., Wu, D., Xiu, W., Huang, Z., 2019. A carpool matching model with both  
1092 social and route networks. *Computers, Environment and Urban Systems* 75, 90–102.  
1093 <https://doi.org/10.1016/j.compenvurbsys.2019.01.008>

1094 Xiao, N., Bennett, D.A., Armstrong, M.P., 2002. Using evolutionary algorithms to generate alternatives  
1095 for multiobjective site-search problems. *Environment and Planning A* 34, 639–656.  
1096 <https://doi.org/10.1068/a34109>

1097 Yamani Douzi Sorkhabi, S., Romero, D.A., Yan, G.K., Gu, M.D., Moran, J., Morgenroth, M., Amon, C.H.,  
1098 2016. The impact of land use constraints in multi-objective energy-noise wind farm layout  
1099 optimization. *Renewable Energy* 85, 359–370. <https://doi.org/10.1016/j.renene.2015.06.026>  
1100 Yao, J., Zhang, X., Murray, A.T., 2018. Spatial Optimization for Land-use Allocation: Accounting for  
1101 Sustainability Concerns. *International Regional Science Review* 41, 579–600.  
1102 <https://doi.org/10.1177/0160017617728551>  
1103 Zhang, F., Zhao, P., Thiyagalingam, J., Kirubarajan, T., 2019. Terrain-influenced incremental  
1104 watchtower expansion for wildfire detection. *Science of The Total Environment* 654, 164–176.  
1105 <https://doi.org/10.1016/j.scitotenv.2018.11.038>  
1106 Zitzler, E., Laumanns, M., Bleuler, S., 2004. A Tutorial on Evolutionary Multiobjective Optimization, in:  
1107 Gandibleux, X., Sevaux, M., Sörensen, K., T'kindt, V. (Eds.), *Metaheuristics for Multiobjective*  
1108 *Optimisation*. Springer Berlin Heidelberg, Berlin, Heidelberg, pp. 3–37.  
1109 [https://doi.org/10.1007/978-3-642-17144-4\\_1](https://doi.org/10.1007/978-3-642-17144-4_1)  
1110